SOLUTE DISPERSION IN GROUNDWATER: THE SYNERGISTIC EFFECT OF HETEROGENEITY AND HYDRAULIC GRADIENT VARIABILITY

by

GREGORY W. COUNCIL

B.S., Civil and Environmental Engineering
Duke University, 1992

Submitted to the Department of Civil and Environmental Engineering
in Partial Fulfillment of the Requirements
for the Degree of

MASTER OF SCIENCE
in Civil and Environmental Engineering

at the

MASSACHUSETTS INSTITUTE OF TECHNOLOGY

September 1994

Signature of Author _____
Department of Civil and Environmental Engineering
August 12, 1994

Certified by _____
Associate Professor Dennis McLaughlin
Thesis Supervisor

Accepted by _____
Joseph M. Sussman
Chairman, Departmental Committee on Graduate Studies

SOLUTE DISPERSION IN GROUNDWATER: THE SYNERGISTIC EFFECT OF HETEROGENEITY AND HYDRAULIC GRADIENT VARIABILITY

by

GREGORY W. COUNCIL

Submitted to the Department of Civil and Environmental Engineering on August 12, 1994
in partial fulfillment of the requirements for the Degree of Master of Science
in Civil and Environmental Engineering

ABSTRACT

Aquifer heterogeneity and temporally variable hydrologic forcing combine to produce field-scale spreading of dissolved groundwater contamination. Stochastic analysis of the groundwater flow and transport processes yields effective parameters (e.g. macrodispersivity) that are useful for the modeling and analysis of contaminant plumes. The development here follows similar studies by *Gelhar and Axness* [1983] and *Rehfeldt and Gelhar* [1990], but differs by retaining an extra term in the Darcy perturbation equation. This term is important when both geologic and hydrologic variability are significant.

The resulting expression for macrodispersivity is a sum of three terms. The first term was derived by *Gelhar and Axness* [1983] and depends on the spatial structure of aquifer hydraulic conductivity. The second term was added by *Rehfeldt and Gelhar* [1990] to show the effect of small temporal perturbations in the hydraulic gradient. The third term is new with this thesis, and depends on both geological variability and variable hydrologic forcing.

Numerical flow modeling demonstrates a procedure for relating hydraulic gradient variability to measurements of boundary conditions (namely, hydraulic head). Two examples are studied at a hypothetical site: one representing an aquifer-connected lake, and one showing the effects of variable inflow from an upgradient recharge zone.

Seasonal periodicity in the hydrologic forcing, manifested in high-frequency energy of the hydraulic gradient spectrum, is shown to have a significant effect on the transverse and off-diagonal components of the macrodispersivity tensor. For a nominal case, with typical physical parameters, the transverse horizontal macrodispersivity prediction made here is significantly higher than in the previous studies, and is roughly one order of magnitude less than the longitudinal dispersivity. This ratio of transverse to longitudinal dispersivity is in agreement with field values obtained from concentration measurements.

Supervisor: Dr. Dennis McLaughlin
Title: Associate Professor of Civil and Environmental Engineering

ACKNOWLEDGMENTS

I would like to thank my advisor and editor Dr. Dennis McLaughlin. Dennis has made me think about things in new ways and has been patient and helpful as I struggled to grasp difficult concepts and produce tangible results. In short, he has been an excellent educator.

I am grateful for my friends at the Parsons Lab, who make work a pleasant experience, and for my roommates and friends, Kory and Susan, who make our apartment feel like home. Special thanks goes to Lynn Reid for her advice and informal tutoring, and to Kathy Hess for helping me obtain the data for Appendix C.

Most of all, I thank my family, especially my parents, for teaching, supporting, and loving me all the days of my life.

With gratitude, I acknowledge the support of the Parsons Foundation and the National Science Foundation (Grant No. EAR-9218602, Topic: "An investigation of hydrologic scale: Natural Variability, Modeling, and Data Collection"). I also thank Dr. David Marks for helping me get started at MIT.

TABLE OF CONTENTS

LIST OF FIGURES

LIST OF TABLES

1. INTRODUCTION AND BACKGROUND

Groundwater is an important natural resource. The subsurface environment stores and transports much of the earth's water taking infiltration to plants, lakes, and oceans. Humans dig wells to tap this resource for irrigation and personal consumption. Contamination from surficial and buried sources can leach into the groundwater and move along with it, often threatening water supply wells or other environmental receptors. The movement of contaminants underground is difficult to predict, partly because of the high variability in aquifer material.

Since the early 1980s researchers have used stochastic analysis to help understand the effects of aquifer heterogeneity on groundwater flow and dissolved contaminant transport. The methods have a probabilistic base and lead to statistical answers, often an expected, or mean, behavior, and a measure of the degree of uncertainty. For the transport problem, it is important to understand the rate and direction of bulk movement and the degree of spreading of the contaminant plume. At the scale of most contaminant plumes, the groundwater flow field is highly variable from point to point and from time to time. This flow variability leads to a spreading of contamination known as "macrodispersion". Specifically, different parts of the contamination mass move at different velocities and end up farther apart.

The velocity variability that leads to macrodispersion results not only from heterogeneity, but also from variable inflow and outflow patterns determined by regional hydrologic conditions. For instance, as a lake rises in response to increased streamflow, groundwater flowing in a connected aquifer changes direction to flow away from the lake. Such hydrologic forcing conditions exhibit variability and randomness and can also be treated in a stochastic framework.

Engineers develop models and collect data to predict what will happen or what has happened to contaminant plumes. Frequently, they model transport by assuming that the dispersion process is Fickian—that is, mass moves from high concentration areas to low concentration areas. In analyzing data to determine the rate of dispersion, engineers often use the method of moments [*Aris*, 1956] and assume a constant flow velocity for the center of the contaminant plume. Thus, the advection and dispersion parameters are usually empirically-derived from data and simple groundwater models. The goal of much

of stochastic analysis (including this thesis) is to estimate the magnitude of these practical parameters from the underlying geologic and hydrologic conditions.

SPREADING DUE TO HETEROGENEITY IN A STEADY FLOW FIELD

Gelhar and Axness [1983] used stochastic techniques to study plume spreading in a heterogeneous aquifer. They applied well-established physical laws of flow and transport at the small (local) scale and averaged with known (or assumed) ensemble statistics for hydraulic conductivity. Ergodicity was assumed, making the ensemble averages appropriate measures of large (field) scale behavior. In the analysis, the large scale average hydraulic gradient and mean flow vectors were assumed to be constant.

Gelhar and Axness based their study on three basic relationships: the advection-dispersion equation (conservation of solute mass), the continuity equation (conservation of total mass) and Darcy's Law (empirical momentum conservation). Applying these relationships at the local scale and averaging leads to mean flow and transport equations. The mean equations have the same form as the corresponding local equations, with additional "closure" terms that depend on correlations between random variables (e.g. velocity and concentration). Using perturbation analysis, the closure terms are simplified and effective parameters (e.g. macrodispersivity, effective conductivity) are derived.

By assuming a locally linear mean concentration profile, *Gelhar and Axness* arrived at a Fickian type of macrodispersion that is (at large time) proportional to the mean concentration gradient. Dividing the proportionality constant by the mean velocity yields the macrodispersivity tensor, A, that is the focus of this work.

Applying their analysis in a three-dimensional isotropic conductivity field, *Gelhar and Axness* (equation 37) determined that longitudinal macrodispersivity is proportional to the correlation length scale of hydraulic conductivity while the two transverse dispersivities are proportional to the local dispersivities. The difference between the predictions for longitudinal and transverse macrodispersivity is usually several orders of magnitude. Since the conductivity correlation length is problem scale-dependent [*Gelhar*, 1986, Figure 8], the longitudinal dispersivity is predicted to be proportional to the scale of the study. On the other hand, the transverse dispersivities predicted by the *Gelhar and Axness* are independent of problem scale.

Observed horizontal transverse dispersivities are usually only one or two orders of magnitude smaller than longitudinal dispersivities and are somewhat scale-dependent [*Gelhar et. al*, 1992]. *Gelhar and Axness* achieved higher transverse dispersivities by treating an anisotropic conductivity field oriented at an angle to the hydraulic gradient.

ENHANCED SPREADING IN A VARYING FLOW FIELD

Several researchers [e.g. *Naff et. al*, 1989, *Rehfeldt and Gelhar*, 1992, *Kinzelbach and Ackerer*, 1986, and *Goode and Konikow*, 1990] have suggested that unsteady flow could lead to enhanced plume spreading. This thesis extends the study of variable flow effects on macrodispersivity following procedures similar to *Gelhar and Axness* [1983] and *Rehfeldt and Gelhar* [1992].

Macrodispersivity Resulting From a Time-Random Hydraulic Gradient

Rehfeldt and Gelhar followed up on the *Gelhar and Axness* study by including a temporally variable hydraulic gradient. They represented the gradient of the hydraulic head by three terms (their equation 16): an ensemble mean hydraulic gradient which is constant in time and space, a spatially uniform, temporally variable term, and a residual term that is variable in time and space. A similar, more explicit representation is made in Section 2 of this thesis.

Rehfeldt and Gelhar considered the temporal forcing in the hydraulic gradient to be a small perturbation in time about the mean gradient, J, and came up with an extra term in the macrodispersivity expression. This added term represents the dispersivity due strictly to gradient fluctuations and is independent of aquifer heterogeneity. The *Rehfeldt and Gelhar* macrodispersivity term would apply even for a homogeneous medium.

Interestingly, the *Rehfeldt and Gelhar* result shows no effect for periodic gradient forcing. Thus the result shows no contribution to contaminant spreading from seasonal hydrologic changes. *Rehfeldt and Gelhar* studied only a Markov type of gradient process where the auto-correlation decreases monotonically with time lag.

Apparent Dispersivity Due to Deterministic, Periodic Gradient Shifts

Goode and Konikow simulated the effect of a flow vector that changed direction, discretely, in time. They convolved two solutions for a pulse-source plume to show the

effect of alternating the flow direction from an angle θ to $-\theta$ with the primary axis. This periodic direction change leads to a plume that is wider than one travelling along a straight path (see Figure 1.1).

Goode and Konikow showed that the plume resulting from this type of flow cycle could also be described by a plume travelling along the primary axis at a slower velocity and with different dispersivities. The velocities and dispersivities needed to fit the actual plume with the constant-direction plume were termed "apparent" parameters. *Goode and Konikow*'s Figures 2 and 3 show how apparent dispersivities relate to the amount of flow variability, θ, and the actual ratio of transverse to longitudinal dispersivity. The plots show that the apparent transverse dispersivity can be markedly higher than the actual transverse dispersivity, while the longitudinal dispersivity changes less. The *Goode and Konikow* analysis does not, however, address the possible interplay between geologic variability and periodic hydraulic forcing.

THESIS SCOPE

The analysis presented here uses stochastic techniques to show how hydraulic gradient variability and aquifer heterogeneity have a synergistic effect on macrodispersion. The two terms produced in the *Gelhar and Axness* and *Rehfeldt and Gelhar* studies do not fully characterize macrodispersivity in an unsteady flow field, especially when there is a significant periodic (seasonal) component to the hydrologic variability. This thesis expands the *Rehfeldt and Gelhar* work by keeping an extra term in the Darcy equation; this term represents the interplay between geologic and hydrologic variability and can be large if the gradient is highly variable.

Also, this thesis shows how regional hydrologic variability causes variability in the aquifer hydraulic gradient. A hypothetical site is studied to show how the hydraulic gradient responds to varying flow boundaries. A numerical flow model relates the statistics of the gradient to hydraulic head statistics at the regional boundary.

The next section begins with the local flow and transport equations and concludes with a general expression for macrodispersivity. Section 3 shows the effects of regional hydrologic changes on the hydraulic gradient, and Section 4 ties the other sections together, giving macrodispersivity values under different geologic and hydrologic conditions.

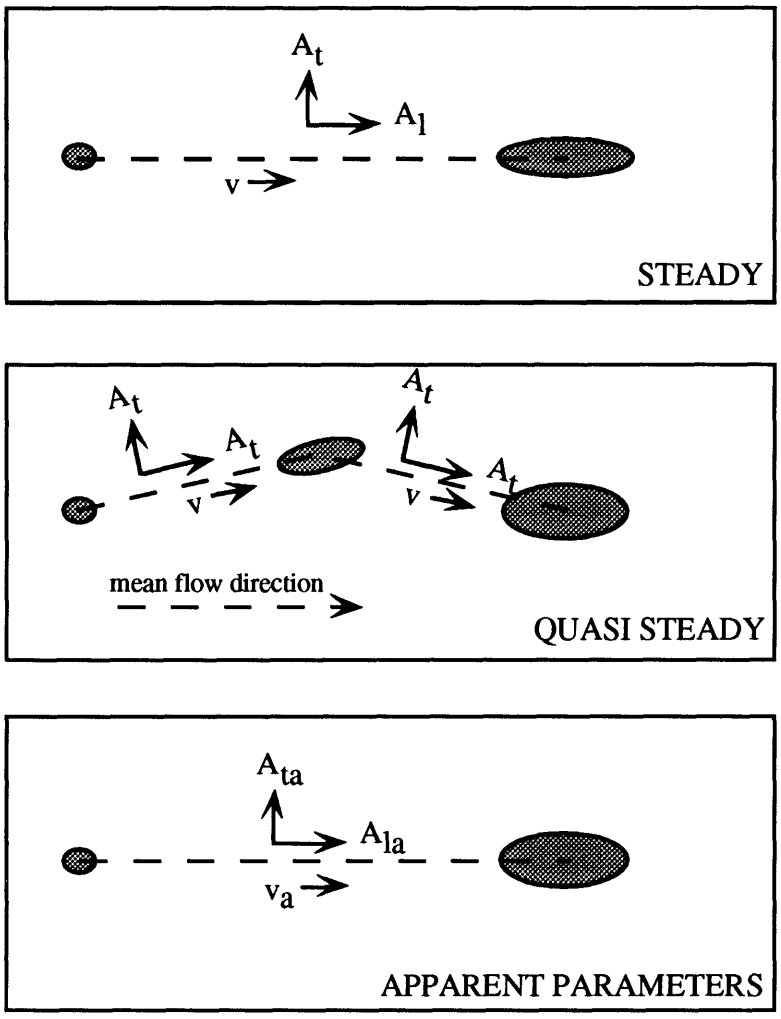

Figure 1.1 "Apparent" dispersion in a quasi-steady flow field, as explained by *Goode and Konikow* [1990]. The constant parameters A_{la} and A_{ta} model the apparent effect of dispersivities and velocities acting at an angle to the mean flow direction. The result of the quasi-steady flow field is a wider plume (given that A_l is larger than A_t).

2. FORMULATION AND ANALYSIS

This section establishes the framework for the stochastic analysis, lists the major assumptions, develops solutions to the stochastic differential equations, and concludes with a general expression for macrodispersivity.

We begin by stating the equations that govern groundwater flow and transport. Noting that there are two sources of variability, geologic heterogeneity and hydrologic forcing fluctuations, we take averages over one or both of the random variables to derive mean and perturbation equations. We solve for the perturbed quantities using stationary theory and Fourier variable representations. The macrodispersivity is then expressed in terms of the log-conductivity and hydraulic gradient spectra.

BASIC CONCEPTS AND GOVERNING EQUATIONS

At the local scale, the movement of an ideal, conservative solute is governed by the advection-dispersion equation:

$$n\frac{\partial c(\mathbf{x},t)}{\partial t} = \frac{\partial}{\partial x_i}\left[E_{ij}\frac{\partial c(\mathbf{x},t)}{\partial x_j} - c(\mathbf{x},t)q_i(\mathbf{x},t)\right] \tag{2.1}$$

where c is the solute concentration (M/L^3), n is the porosity, E_{ij} is the local dispersion tensor (L^2/T), and q_i is the specific discharge vector or Darcy velocity (L/T).

The specific discharge is determined from Darcy's Law:

$$q_i(\mathbf{x},t) = -K(\mathbf{x})\frac{\partial h(\mathbf{x},t)}{\partial x_i} \tag{2.2}$$

where K is the hydraulic conductivity (L/T) and h is the hydraulic head (L). Equation (2.2) applies for a locally isotropic medium.

Conservation of fluid mass is expressed by the continuity equation:

$$S_s\frac{\partial h(\mathbf{x},t)}{\partial t} + \frac{\partial q_i(\mathbf{x},t)}{\partial x_i} = 0 \tag{2.3a}$$

where S_s is the specific storage of the medium (L^{-1}). To simplify this analysis the aquifer storage is taken to be negligible ($S_s \equiv 0$). The continuity equation is then

$$\frac{\partial q_i(\mathbf{x},t)}{\partial x_i} = 0 \tag{2.3b}$$

This corresponds to the quasi-steady condition imposed by *Rehfeldt and Gelhar* and *Goode and Konikow*.

To understand the expected behavior of the solute concentration at the scale of a contaminant plume, the local-scale equations (2.1), (2.2), and (2.3b) are analyzed in a stochastic framework with appropriate boundary conditions.

TRANSPORT DESCRIPTION

The local solute concentration and velocity variables are each expressed as an ensemble (grand) mean and a perturbation:

$$c(\mathbf{x},t) = \bar{c}(\mathbf{x},t) + c'(\mathbf{x},t) \tag{2.4}$$

$$q_i(\mathbf{x},t) = \overline{q_i}(\mathbf{x},t) + q_i'(\mathbf{x},t) \tag{2.5}$$

Expanding the transport equation (2.1) and the continuity equation (2.3b) in terms of these means and perturbations gives

$$n\frac{\partial \bar{c}}{\partial t} + n\frac{\partial c'}{\partial t} = \frac{\partial}{\partial x_i}\left[E_{ij}\frac{\partial \bar{c}}{\partial x_j} + E_{ij}\frac{\partial c'}{\partial x_j} - \bar{c}\,\overline{q_i} - c'\overline{q_i} - \bar{c}q_i' - c'q_i'\right] \tag{2.6}$$

and

$$\frac{\partial \overline{q_i}(\mathbf{x},t)}{\partial x_i} + \frac{\partial q_i'(\mathbf{x},t)}{\partial x_i} = 0 \tag{2.7}$$

Taking the expected value of (2.7) and subtracting it from the total equation confirms that

$$\frac{\partial \overline{q_i}(\mathbf{x},t)}{\partial x_i} = 0; \quad \frac{\partial q_i'(\mathbf{x},t)}{\partial x_i} = 0 \tag{2.8}$$

Using these equations and assuming constant local dispersion, the mean transport equation is

$$n\frac{\partial \bar{c}}{\partial t}+\bar{q}_i\frac{\partial \bar{c}}{\partial x_i}-E_{ij}\frac{\partial \bar{c}}{\partial x_i \partial x_j}=-\frac{\partial}{\partial x_i}\left(\overline{c'q'_i}\right) \tag{2.9}$$

where the term $\overline{c'q'_i}$ is the macrodispersive flux of interest in this study. This term represents the large scale correlation of concentration and velocity perturbations. To obtain an equation for the concentration perturbation appearing in this term, equation (2.9) is subtracted from (2.6) to yield

$$n\frac{\partial c'}{\partial t}+\bar{q}_i\frac{\partial c'}{\partial x_i}-E_{ij}\frac{\partial c'}{\partial x_i \partial x_j}=-q'_j\frac{\partial \bar{c}}{\partial x_j}=G_j q'_j \tag{2.10}$$

The concentration gradient, $G_j=-\partial\bar{c}/\partial x_j$, is assumed to be approximately constant at the local scale, where equation (2.10) is applied (this simplification is also made in *Gelhar and Axness* and *Rehfeldt and Gelhar*). In other words, the mean concentration profile is approximated by a straight line at the scale of concentration perturbations. If this holds, then the macrodispersive flux, $\overline{c'q'_i}$, is later shown to be proportional to the mean concentration gradient and the closure term in (2.9) has the same form as the local (Fickian) dispersion term on the left-hand-side of (2.9). Although this approximation can be quite severe, especially at the edges of a contamination plume, it is practical given that modelers and analysts almost universally use an equation of the form

$$n\frac{\partial \bar{c}}{\partial t}+\bar{q}_i\frac{\partial \bar{c}}{\partial x_i}-qA_{ij}\frac{\partial \bar{c}}{\partial x_i \partial x_j}=0 \tag{2.11}$$

to describe field scale contaminant spreading (q is the Darcy velocity magnitude). Using a constant local concentration gradient facilitates the derivation of an expression for A_{ij}.

The concentration perturbation equation (2.10) can be solved once expressions for $\bar{q}_i(\mathbf{x},t)$ and $q'_i(\mathbf{x},t)$ are obtained, for that purpose, we turn to a stochastic description of groundwater flow.

FLOW DESCRIPTION

Head Equations

The flow problem can be completely described by combining the continuity equation (2.3b) with the Darcy equation (2.2) and imposing boundary conditions. For a

case where the head is specified everywhere along the boundary (∂D), the flow equations are:

$$\frac{\partial}{\partial x_i}\left[K(\mathbf{x})\frac{\partial h(\mathbf{x},t)}{\partial x_i}\right]=0 \quad \in D \tag{2.12a}$$

$$h(\mathbf{x},t)=H(\mathbf{x},t) \quad \in \partial D \tag{2.12b}$$

Here, the spatial domain D corresponds to the regional scale, with the temporally variable boundary head given by H. Note that this analysis could be extended without great difficulty to include specified flux conditions; confining the present discussion to prescribed head boundaries illustrates the major points more simply. It is assumed that the region of interest (i.e. the location of the contaminant plume) is located far from the boundaries.

Expanding equation (2.12a) and simplifying yields

$$\frac{\partial f(\mathbf{x})}{\partial x_i}\frac{\partial h(\mathbf{x},t)}{\partial x_i}+\frac{\partial^2 h(\mathbf{x},t)}{\partial x_i\,\partial x_i}=0 \quad \in D \tag{2.13a}$$

$$h(\mathbf{x},t)=H(\mathbf{x},t) \quad \in \partial D \tag{2.13b}$$

with the log-conductivity, f, defined by

$$f(\mathbf{x})=\ln\left(K(\mathbf{x})/K_0\right) \tag{2.14}$$

(K_0 is a constant usually taken to be unity). Equations (2.13) show that h is a function of two independent variables: the log-conductivity and the boundary head.

The log-conductivity is assumed to be a spatially stationary stochastic random variable (i.e. its statistical moments are translation invariant) and can be written in terms of its constant mean and local perturbation:

$$f(\mathbf{x})=\overline{f}+f'(\mathbf{x}) \tag{2.15}$$

To isolate the effect of the time-varying boundary conditions, we would like to take the expected value of (2.13) with respect to the random variable f only. Defining the f-expectation of the aquifer head as shown in Table 2.1 leads to the following decomposition:

Table 2.1 Expectations and Perturbations

Notation	*Definition/Terminology*
p_f	ensemble probability density function of the random log-conductivity, f
p_b	ensemble probability density function of the random boundary head, H
$E_f[h(\mathbf{x},t)]$	$\int h\left(\mathbf{x},t\middle\|\hat{f},H\right)p_f\left(\hat{f}\right)d\hat{f}$; f-expectation of head
$\overline{h}(\mathbf{x},t)$ or $E_{fb}[h(\mathbf{x},t)]$	$\int h\left(\mathbf{x},t\middle\|\hat{f},\hat{H}\right)p_f\left(\hat{f}\right)p_b\left(\hat{H}\right)d\hat{f}\,d\hat{H}$; grand mean
$h'(\mathbf{x},t)$	$h(\mathbf{x},t)-\overline{h}(\mathbf{x},t)$; total perturbation
$h'_f(\mathbf{x},t)$	$h(\mathbf{x},t)-E_f[h(\mathbf{x},t)]$; f-perturbation
$h'_b(\mathbf{x},t)$	$E_f[h(\mathbf{x},t)]-\overline{h}(\mathbf{x},t)$
$-E_f\left[\dfrac{\partial h(\mathbf{x},t)}{\partial x_i}\right]$	$J_i(t)$; hydraulic gradient
$-\dfrac{\partial \overline{h}(\mathbf{x},t)}{\partial x_i}$	$\overline{J_i}$; mean hydraulic gradient
$-\dfrac{\partial h'_b(\mathbf{x},t)}{\partial x_i}$	$J'_{bi}(t)$; temporal gradient fluctuation

Useful Identities

$E_f[f(\mathbf{x})]=\overline{f}$	$E_f[H(\mathbf{x},t)]=H(\mathbf{x},t)$
$E_f[f'(\mathbf{x})]=0$	$E_f\left[h'_f(\mathbf{x},t)\right]=0$
$h=\overline{h}+\left(h-E_f[h]\right)+\left(E_f[h]-\overline{h}\right)$ $=\overline{h}+h'_f+h'_b$	$h'(\mathbf{x},t)=h'_f(\mathbf{x},t)+h'_b(\mathbf{x},t)$
$\dfrac{\partial h(\mathbf{x},t)}{\partial x_i}=-\overline{J_i}-J'_{bi}(t)+\dfrac{\partial h'_f(\mathbf{x},t)}{\partial x_i}$	$J_i(t)=\overline{J_i}+J'_{bi}(t)$

$$h(\mathbf{x},t) = E_f[h(\mathbf{x},t)] + h'_f(\mathbf{x},t) \tag{2.16}$$

Thus, the expected value of (2.13) with respect to f only is

$$\frac{\partial^2 E_f[h]}{\partial x_i \partial x_i} = -E_f\left[\frac{\partial f'}{\partial x_i}\frac{\partial h'_f}{\partial x_i}\right] \quad \in D \tag{2.17a}$$

$$E_f[h] = H(\mathbf{x},t) \quad \in \partial D \tag{2.17b}$$

(note that $\overline{f}$ is spatially uniform). Since the imposed head boundaries are independent of the conductivity field, the f-expectation of h is exactly H on the boundary. It is assumed (and later verified) that the second-order perturbation term on the right hand side of (2.17a) is zero, leading to a Laplacian expression for the f-expectation of head:

$$\frac{\partial^2 E_f[h]}{\partial x_i \partial x_i} = 0 \quad \in D; \quad E_f[h] = H \quad \in \partial D \tag{2.18}$$

In general, the solution for this boundary-value problem can be written in terms of the Green's Function of the Laplacian, G, and the boundary conditions.

$$E_f[h(\mathbf{x},t)] = \int_{\partial D} \frac{\partial G(\mathbf{x},\xi)}{\partial \xi_i} n_i H(\xi,t)\, d\xi \tag{2.19}$$

(n_i is the unit vector normal to ∂D). In this form, it is shown that the f-expectation of head at every location depends on the head imposed at every point along the boundary.

Subtracting (2.17) from (2.13) and ignoring products of perturbed terms gives the following first-order perturbation (in f) equations of flow:

$$\frac{\partial^2 h'_f}{\partial x_i \partial x_i} - J_i \frac{\partial f'}{\partial x_i} = 0 \quad \in D \tag{2.20a}$$

$$h'_f = 0 \quad \in \partial D \tag{2.20b}$$

with the f-expected head gradient (hereafter referred to simply as the "hydraulic gradient"), J_i, defined by

$$J_i(\mathbf{x},t) = -E_f\left[\frac{\partial h(\mathbf{x},t)}{\partial x_i}\right] \tag{2.21}$$

Differentiation of equation (2.19) shows that J_i depends on the boundary condition H, which is variable (and random) in time.

Equation (2.20a) can be evaluated using stationary theory if the hydraulic gradient is spatially uniform over the plume region (a function of time only: $J_i(t)$). We assume that the boundary condition is far enough from the region of interest to give such a effect. The hydraulic gradient, $J_i(t)$, is therefore considered to be a statistically homogeneous stochastic random variable in time (independent of f and the exact location of the boundaries). Referring to Table 1.2, the hydraulic gradient is written as:

$$J_i(t) = \overline{J_i} + J'_{bi}(t) \tag{2.22}$$

where $\overline{J_i}$ and $J'_{bi}(t)$ are defined as:

$$\overline{J_i} = -\frac{\partial \overline{h}(\mathbf{x},t)}{\partial x_i} \tag{2.23}$$

$$J'_{bi}(t) = -\frac{\partial h'_b(\mathbf{x},t)}{\partial x_i} \tag{2.24}$$

and we have used the identity $E_f\left[h'_f(\mathbf{x},t)\right] \equiv 0$

Far from the boundaries, equations (2.20) are not sensitive to the boundary conditions (2.20b) [*Ababou*, 1988; *Naff and Vecchia*, 1986], and the f-perturbation of head is described by:

$$\frac{\partial^2 h'_f(\mathbf{x},t)}{\partial x_i \partial x_i} - \overline{J_i}\frac{\partial f'(\mathbf{x})}{\partial x_i} - J'_{bi}(t)\frac{\partial f'(\mathbf{x})}{\partial x_i} = 0 \tag{2.25}$$

This differs from *Rehfeldt and Gelhar* (equation 24) because only the expected value with respect to f has been taken (they use the total mean). In cases where the variability of $J_i(t)$ is large, equation (2.25) proves to be a more useful expression.

Velocity Equations

To obtain expressions for the mean and local velocity, we return to the Darcy equation (2.2). Using (2.14) and assuming $f' << 1$, the hydraulic conductivity is approximated by a second-order Taylor series:

$$K(\mathbf{x}) = K_g e^{f'} \cong K_g\left(1 + f'(\mathbf{x}) + \frac{(f'(\mathbf{x}))^2}{2}\right) \tag{2.26}$$

where $K_g = K_0 e^{\overline{f}}$ is the geometric mean of K. Using (2.26) and (2.21), the Darcy velocity is represented in terms of f-expectations and perturbations by:

$$q_i(\mathbf{x},t) = K_g\left(1 + f'(\mathbf{x}) + \frac{(f'(\mathbf{x}))^2}{2}\right)\left(\overline{J_i} + J'_{bi}(t) - \frac{\partial h'_f(\mathbf{x},t)}{\partial x_i}\right) \tag{2.27}$$

The mean equation with respect to f is thus (to second order):

$$E_f[q_i(\mathbf{x},t)] = K_g\left\{\overline{J_i}\left(1 + \frac{\sigma_f^2}{2}\right) + J'_{bi}(t)\left(1 + \frac{\sigma_f^2}{2}\right) - E_f\left[f'(\mathbf{x})\frac{\partial h'_f(\mathbf{x},t)}{\partial x_i}\right]\right\} \tag{2.28}$$

Taking the expectation of this equation with respect to the random boundary conditions, the grand mean is:

$$\overline{q_i}(\mathbf{x},t) = E_{fb}[q_i(\mathbf{x},t)] = K_g\left\{\overline{J_i}\left(1 + \frac{\sigma_f^2}{2}\right) - E_{fb}\left[f'(\mathbf{x})\frac{\partial h'_f(\mathbf{x},t)}{\partial x_i}\right]\right\} \tag{2.29}$$

(note that $E_{fb}[J'_{bi}(t)] = 0$).

Subtracting (2.29) from (2.27) gives the second-order velocity perturbation equation:

$$\begin{aligned} q'_i = K_g\Bigg[&\overline{J_i}\left(f' + \frac{f'^2 - \sigma_f^2}{2}\right) + J'_{bi}\left(1 + f' + \frac{f'^2}{2}\right) \\ &- \frac{\partial h'_f}{\partial x_i} - f'\frac{\partial h'_f}{\partial x_i} + E_{fb}\left[f'\frac{\partial h'_f}{\partial x_i}\right]\Bigg] \end{aligned} \tag{2.30}$$

In the Taylor expansion of f', it was assumed that log-conductivity variations were small. This approximation has proven useful even in cases where the hydraulic conductivity varies over an order of magnitude. Keeping this fact in mind, terms in (2.30) that are second order in f' are ignored (also, the last two terms in (2.30) are assumed to approximately cancel each other). But in certain field situations it is expected

that the time perturbation of the hydraulic gradient (J'_{bi}) will not be small compared to its mean. Therefore, the simplified mean-removed Darcy equation is

$$q'_i(\mathbf{x},t) = K_g\left(\overline{J}_i f'(\mathbf{x}) + J'_{bi}(t) + J'_{bi}(t)f'(\mathbf{x}) - \frac{\partial h'_f(\mathbf{x},t)}{\partial x_i}\right) \tag{2.31}$$

Equation (2.31) is the same as in *Rehfeldt and Gelhar* (equation 19) but with the $J'_{bi}f'$ term retained. The term $J'_{bi}f'$ is kept because 1) its contribution is expected to be significant in cases where the field gradient varies significantly, 2) it quantifies the synergistic effect of random conductivity and random hydraulic forcing, and 3) its evaluation requires only a slight modification of first-order solution techniques.

VARIABLE REPRESENTATION

The two sources of uncertainty, $f'(\mathbf{x})$ and $J'_{bi}(t)$ are now expressed in a manner that facilitates the solution of the perturbation equations. The first independent stochastic random variable, the time invariant log-conductivity fluctuation $f'(\mathbf{x})$, is written in terms of a Fourier series of random increments in the wave number domain [*Papoulis*, 1984, p. 306]:

$$f'(\mathbf{x}) = \int W_f(\mathbf{k}) e^{i\mathbf{k}\cdot\mathbf{x}}\, d\mathbf{k} = \int W_f^*(\mathbf{k}) e^{-i\mathbf{k}\cdot\mathbf{x}}\, d\mathbf{k} \tag{2.32}$$

where $\mathbf{k}$ is the wave number vector (L^{-1}), $i = \sqrt{-1}$, and W_f is the random Fourier amplitude of f', with its complex conjugate denoted by W_f^*. The properties of W_f are:

$$W_f(\mathbf{k}) = (2\pi)^N \int f'(\mathbf{x}) e^{-i\mathbf{k}\cdot\mathbf{x}}\, d\mathbf{x} \tag{2.33a}$$

$$E\left[W_f(\mathbf{k})\right] = (2\pi)^N \int E\left[f'(\mathbf{x})\right] e^{-i\mathbf{k}\cdot\mathbf{x}}\, d\mathbf{x} \equiv 0 \tag{2.33b}$$

$$E\left[W_f(\mathbf{k}) W_f^*(\mathbf{k}')\right] = S_{ff}(\mathbf{k})\,\delta(\mathbf{k}-\mathbf{k}') \tag{2.33c}$$

where N is the spatial dimensionality of the problem (1, 2, or 3) and S_{ff} is the log-conductivity spectrum. Because f' is independent of time, it can also be represented by

$$f'(\mathbf{x}) = \iint W_f(\mathbf{k})\,\delta(\omega) e^{i(\mathbf{k}\cdot\mathbf{x}+\omega t)}\, d\mathbf{k}\, d\omega \tag{2.34}$$

with angular frequency ω (radians/T).

The other independent stochastic random variable, the spatially invariant hydraulic gradient fluctuation $J'_{bi}(t)$, is represented by

$$J'_i(t) = \int W_{J_i}(\omega)\, e^{i\omega t}\, d\omega = \iint W_{J_i}(\omega)\delta(\mathbf{k}) e^{i(\mathbf{k}\cdot\mathbf{x}+\omega t)}\, d\mathbf{k}\, d\omega \tag{2.35}$$

The form of the perturbation equations yields dependent variables that are space-time stationary random variables. They are represented with random amplitudes that can depend on wave number and frequency:

$$h'_f(\mathbf{x},t) = \iint W_h(\mathbf{k},\omega)\, e^{i(\mathbf{k}\cdot\mathbf{x}+\omega t)}\, d\mathbf{k}\, d\omega \tag{2.36}$$

$$q'_i(\mathbf{x},t) = \iint W_{q_i}(\mathbf{k},\omega)\, e^{i(\mathbf{k}\cdot\mathbf{x}+\omega t)}\, d\mathbf{k}\, d\omega \tag{2.37}$$

$$c'(\mathbf{x},t) = \iint W_c(\mathbf{k},\omega)\, e^{i(\mathbf{k}\cdot\mathbf{x}+\omega t)}\, d\mathbf{k}\, d\omega \tag{2.38}$$

(note that for h we are interested in the perturbation with only its f-expectation removed). Using these variable representations in equations (2.10), (2.25), and (2.31) gives expressions for the dependent variable perturbations in terms of the independent variable perturbations. Spectral representation is then invoked to give expressions for mean parameters such as $\overline{q_i}$ and the quantity of interest, $\overline{c'q'_i}$.

MACRODISPERSIVE FLUX

Recalling the transport perturbation equation, (2.10), and using the variable representations in (2.37) and (2.38) leads to

$$\begin{aligned}\iint e^{i(\mathbf{k}\cdot\mathbf{x}+\omega t)}\Big\{&ni\omega\, W_c(\mathbf{k},\omega) + ik_i\overline{q_i}\, W_c(\mathbf{k},\omega) + k_i k_j E_{ij} W_c(\mathbf{k},\omega) \\ &-G_j\, W_{q_j}(\mathbf{k},\omega)\Big\} d\mathbf{k}\, d\omega = 0\end{aligned} \tag{2.39}$$

which is non-trivial only if the sum in braces is zero. Thus the random amplitudes of concentration are related to those of the velocity by

$$W_c(\mathbf{k},\omega) = \frac{G_j\, W_{q_j}(\mathbf{k},\omega)}{ni\omega + ik_i\overline{q_i} + k_i k_j E_{ij}} \tag{2.40}$$

The mean macrodispersive flux term $\overline{c'q_i'}$ is evaluated using spectral representation:

$$\overline{c'q_i'} = E\left[\iint W_c(\mathbf{k},\omega)e^{i(\mathbf{k}\cdot\mathbf{x}+\omega t)}d\mathbf{k}\,d\omega \iint W_{q_i}^*(\mathbf{k}',\omega')e^{-i(\mathbf{k}'\cdot\mathbf{x}+\omega' t)}d\mathbf{k}'\,d\omega'\right] \quad (2.41a)$$

$$\overline{c'q_i'} = \int\int\int\int \frac{G_j}{ni\omega + ik_i\overline{q_i} + k_ik_jE_{ij}} \overline{W_{q_j}(\mathbf{k},\omega)W_{q_i}^*(\mathbf{k}',\omega')}\,d\mathbf{k}\,d\omega\,d\mathbf{k}'\,d\omega' \quad (2.41b)$$

$$\overline{c'q_i'} = G_j \int\int \frac{S_{q_iq_j}(\mathbf{k},\omega)}{ni\omega + ik_i\overline{q_i} + k_ik_jE_{ij}} d\mathbf{k}\,d\omega \quad (2.41c)$$

which is consistent with *Rehfeldt and Gelhar*'s macrodispersive flux development (equations 13 and 14).

VELOCITY SPECTRUM

The velocity spectrum in (2.41c) is derived from the spectra of the log-conductivity and the hydraulic gradient via the head and velocity perturbation equations. Substituting (2.34), (2.35), and (2.36) into (2.25) gives

$$\iint e^{i(\mathbf{k}\cdot\mathbf{x}+\omega t)}\left\{-k^2W_h(\mathbf{k},\omega) - ik_i\overline{J_i}W_f(\mathbf{k})\delta(\omega) - ik_iW_f(\mathbf{k})W_{J_i}(\omega)\right\}d\mathbf{k}\,d\omega = 0 \quad (2.42)$$

which leads to the relationship:

$$W_h(\mathbf{k},\omega) = -\frac{ik_i}{k^2}\overline{J_i}W_f(\mathbf{k})\delta(\omega) - \frac{ik_i}{k^2}W_f(\mathbf{k})W_{J_i}(\omega) \quad (2.43)$$

where $k^2 = k_1^2 + k_2^2 + k_3^2$ in three dimensions.

Substituting the Fourier variable representations into the Darcy perturbation equation, (2.31), yields

$$\iint e^{i(\mathbf{k}\cdot\mathbf{x}+\omega t)}\left\{W_{q_i}(\mathbf{k},\omega) - K_g\left[\overline{J_i}W_f(\mathbf{k})\delta(\omega) + W_{J_i}(\omega)\delta(\mathbf{k}) + W_{J_i}(\omega)W_f(\mathbf{k}) - ik_iW_h(\mathbf{k},\omega)\right]\right\}d\mathbf{k}\,d\omega = 0 \quad (2.44)$$

Using (2.43), the velocity amplitudes are expressed in terms of the amplitudes of the independent variables, f' and J_i':

$$\begin{aligned} W_{q_i}(\mathbf{k},\omega) &= K_g\left[\overline{J_i}W_f(\mathbf{k})\delta(\omega)+W_{J_i}(\omega)\delta(\mathbf{k})+W_{J_i}(\omega)W_f(\mathbf{k})-ik_iW_h(\mathbf{k},\omega)\right] \\ &= K_g\left[\overline{J_l}\delta(\omega)\left(\delta_{il}-\frac{k_ik_l}{k^2}\right)W_f(\mathbf{k})+W_{J_i}(\omega)\delta(\mathbf{k})\right. \\ &\quad \left.+\left(\delta_{il}-\frac{k_ik_l}{k^2}\right)W_{J_l}(\omega)W_f(\mathbf{k})\right] \end{aligned} \tag{2.45}$$

The term $\overline{W_{q_i}W_{q_j}^*}$ needed in (2.41b) is found by applying spectral representation to (2.45), taking the independence of W_f and W_J into account:

$$\begin{aligned} &\overline{W_{q_i}(\mathbf{k},\omega)W_{q_j}^*(\mathbf{k}',\omega')} \\ &= K_g^2\left[\overline{J_l}\,\overline{J_m}\left(\delta_{il}-\frac{k_ik_l}{k^2}\right)\left(\delta_{jm}-\frac{k_jk_m}{k^2}\right)\delta(\omega)\delta(\omega')S_{ff}(\mathbf{k})\delta(\mathbf{k}'-\mathbf{k})\right. \\ &\quad +\delta(\mathbf{k})\delta(\mathbf{k}')S_{J_iJ_j}(\omega)\delta(\omega'-\omega) \\ &\quad \left.+\left(\delta_{il}-\frac{k_ik_l}{k^2}\right)\left(\delta_{jm}-\frac{k_jk_m}{k^2}\right)S_{J_lJ_m}(\omega)S_{ff}(\mathbf{k})\delta(\mathbf{k}'-\mathbf{k})\delta(\omega'-\omega)\right] \end{aligned} \tag{2.46}$$

Thus the velocity spectrum in (2.41c) is

$$\begin{aligned} S_{q_iq_j}(\mathbf{k},\omega) &= K_g^2\left[\overline{J_l}\,\overline{J_m}\left(\delta_{il}-\frac{k_ik_l}{k^2}\right)\left(\delta_{jm}-\frac{k_jk_m}{k^2}\right)\delta(\omega)S_{ff}(\mathbf{k})\right. \\ &\quad \left.+S_{J_iJ_j}(\omega)\delta(\mathbf{k})+\left(\delta_{il}-\frac{k_ik_l}{k^2}\right)\left(\delta_{jm}-\frac{k_jk_m}{k^2}\right)S_{J_lJ_m}(\omega)S_{ff}(\mathbf{k})\right] \end{aligned} \tag{2.47}$$

which differs from *Rehfeldt and Gelhar* (equation 29). In (2.47) the term that contains the product of the gradient and log-conductivity spectra can be important for a heterogeneous aquifer with significant gradient variability.

General Expression for Macrodispersivity

Searching for a Fickian type of macrodispersivity A_{ij} which satisfies

$$\overline{c'q_i'} = qA_{ij}G_j \tag{2.48}$$

(where q is the magnitude of the mean discharge) equation (2.41c) is rewritten as:

$$A_{ij} = \frac{1}{q}\int\int \frac{S_{q_i q_j}(\mathbf{k},\omega)}{ni\omega + ik_i\overline{q_i} + k_i k_j E_{ij}}\, d\mathbf{k}\, d\omega \tag{2.49}$$

which is equivalent to the macrodispersivity expression in *Rehfeldt and Gelhar* (equation 14).

Substituting the derived velocity spectrum, (2.47), into this macrodispersivity expression results in

$$\begin{aligned} A_{ij} = {} & \frac{K_g^2}{q}\int \frac{\overline{J_l}\,\overline{J_m}}{ik_i\overline{q_i} + k_i k_j E_{ij}}\left(\delta_{il} - \frac{k_i k_l}{k^2}\right)\left(\delta_{jm} - \frac{k_j k_m}{k^2}\right) S_{ff}(\mathbf{k})\, d\mathbf{k} \\ & + \frac{K_g^2}{q}\int \frac{S_{J_i J_j}(\omega)}{ni\omega}\, d\omega \\ & + \frac{K_g^2}{q}\int \left(\delta_{il} - \frac{k_i k_l}{k^2}\right)\left(\delta_{jm} - \frac{k_j k_m}{k^2}\right)\left\{\int \frac{S_{J_l J_m}(\omega)}{ni\omega + ik_i\overline{q_i} + k_i k_j E_{ij}}\, d\omega\right\} S_{ff}(\mathbf{k})\, d\mathbf{k} \end{aligned} \tag{2.50a}$$

The first of the three terms in (2.50) is the macrodispersivity due only to the heterogeneity of the aquifer material. That term is independent of the amount of gradient variability and is equivalent to the macrodispersivity derived in *Gelhar and Axness* (equation 62). The second term is equivalent to the transient macrodispersivity in *Rehfeldt and Gelhar* (equation 34) which is independent of the amount of heterogeneity. The last term is dependent on the variability (spectra) of both the log-conductivity and the hydraulic gradient. It arises because of the extra term ($J_i' f'$)retained in the Darcy perturbation equation. The three terms of (2.50) will be referenced as follows (with superscript s for dependence on spatial variability and t for dependence on temporal variability):

$$A_{ij}(\mathbf{x},t) = A_{ij}^{(s)}(\mathbf{x}) + A_{ij}^{(t)}(t) + A_{ij}^{(st)}(\mathbf{x},t) \tag{2.50b}$$

The results of *Gelhar and Axness* and *Rehfeldt and Gelhar* apply for the first two terms, respectively. The third term, $A_{ij}^{(st)}$ is the focus of this work.

EFFECTIVE CONDUCTIVITY AND FLOW CLOSURE TERM

The mean velocity appearing in (2.50) (as q and $\overline{q_i}$) depends on the effective conductivity tensor:

$$\overline{q_i} = \hat{K}_{ij}\overline{J_j} \tag{2.51}$$

To determine the value of $\hat{K}_{ij}$, the second-order perturbation term appearing in the mean velocity equation, (2.28), is evaluated using the Fourier variable representations along with the head amplitude solution, (2.43):

$$\begin{aligned} E_{fb}\left[f'\frac{\partial h'_f}{\partial x_i}\right] &= E_{fb}\left[\int e^{i(\mathbf{k}\cdot\mathbf{x})}W_f(\mathbf{k})d\mathbf{k}\iint ik'_i e^{-i(\mathbf{k}'\cdot\mathbf{x}+\omega' t)}W_h^*(\mathbf{k}',\omega')d\mathbf{k}'\,d\omega'\right] \\ &= \overline{J_j}\int\frac{k_i k_j}{k^2}S_{ff}(\mathbf{k})d\mathbf{k} + \int\int\frac{k_i k_j}{k^2}S_{ff}(\mathbf{k})e^{-i\omega' t}\,\overline{W_{J_j}^*(\omega')}d\mathbf{k}\,d\omega' \\ &= \overline{J_j}\int\frac{k_i k_j}{k^2}S_{ff}(\mathbf{k})d\mathbf{k} \end{aligned} \tag{2.52}$$

which is similar to equation 4.1.49 in *Gelhar* [1993]. Thus the effective conductivity is not altered by gradient variability. In an isotropic, three-dimensional medium, *Gelhar* states that

$$\overline{J_j}\int\frac{k_i k_j}{k^2}S_{ff}(\mathbf{k})d\mathbf{k} = \overline{J_j}\frac{\sigma_f^2}{3}\delta_{ij} \tag{2.53}$$

and the effective conductivity is thus

$$\hat{K}_{ij} = \delta_{ij}K_g\gamma; \quad \gamma \cong 1+\frac{\sigma_f^2}{6} \tag{2.54}$$

where γ is called the flow factor.

Since $\overline{J_i}$ and $\hat{K}_{ij}$ are constants, the mean velocity, $\overline{q_i}$, is also a constant in the mean transport equation and the expression for macrodispersivity. This constant velocity is consistent with the use of standard method-of-moments analyses to predict dispersivity from concentration data.

The second-order closure term in the flow equation is similarly evaluated:

$$E_{fb}\left[\frac{\partial f'}{\partial x_i}\frac{\partial h'_f}{\partial x_i}\right] = -\overline{J_j}\int \frac{k_i^2 k_j}{k^2} S_{ff}(\mathbf{k})\,d\mathbf{k} - \iint \frac{k_i^2 k_j}{k^2} S_{ff}(\mathbf{k})\overline{W^*_{J_j}(\omega')}e^{-i\omega' t}\,d\mathbf{k}\,d\omega'$$
$$= -\overline{J_j}\int \frac{k_i^2 k_j}{k^2} S_{ff}(\mathbf{k})\,d\mathbf{k} = 0 \tag{2.55}$$

(note that the log-conductivity spectrum is even for all k_i), confirming our earlier assumption.

APPROXIMATION OF $A_{ij}^{(st)}$ FOR AN ISOTROPIC MEDIUM

An analytical expression is obtained for $A_{ij}^{(st)}$ in an isotropic medium by ignoring local dispersion. The term of interest, defined in (2.50) is

$$A_{ij}^{(st)} = \frac{K_g^2}{q}\int\left(\delta_{il} - \frac{k_i k_l}{k^2}\right)\left(\delta_{jm} - \frac{k_j k_m}{k^2}\right)\{P_{lm}\}S_{ff}(k)\,d\mathbf{k} \tag{2.56}$$

with

$$P_{lm} = \int_{-\infty}^{\infty} \frac{S_{J_l J_m}(\omega)\,d\omega}{ni\omega + ik_i\overline{q_i} + k_i k_j E_{ij}} \tag{2.57}$$

For an isotropic case, the mean hydraulic gradient will be in the same direction as the mean flow, which defines the x_1 plume axis. Note that the log-conductivity spectrum is a function only of the magnitude of the wave number vector and the magnitude of the mean velocity is given by

$$q = \overline{q_1} \tag{2.58}$$

The P_{lm} integral is solved for the limit as E goes to zero using a method similar to *Rehfeldt and Gelhar* [1992, equations 36-40]. The result is (from Appendix B)

$$P_{lm} = \frac{\pi}{n} S_{J_l J_m}\left(\frac{k_1 q}{n}\right) \tag{2.59}$$

Substitution of (2.59) into (2.56) gives a simplified expression for $A_{ij}^{(st)}$:

$$A_{ij}^{(st)} = \frac{K_g^2 \pi}{nq} \int \left(\delta_{il} - \frac{k_i k_l}{k^2} \right) \left(\delta_{jm} - \frac{k_j k_m}{k^2} \right) S_{J_l J_m} \left(\frac{k_1 q}{n} \right) S_{ff}(k) d\mathbf{k} \qquad (2.60)$$

which can be evaluated analytically or numerically if the statistics of J and f are known.

3. REGIONAL HYDROLOGY AND GRADIENT VARIABILITY

The macrodispersivity expression (2.50) assumes that the gradient spectrum and mean flow magnitude are known. In this section, we examine how the gradient statistics (mean and spectra) needed in equation (2.50) and the effective velocity expression, (2.51), can be calculated from measurements of the boundary conditions.

The horizontal components of the hydraulic gradient at a field site can be estimated from a minimum of three well water levels (four measurements are necessary for a full three-dimensional characterization). Figures 2, 5 and 6 in *Rehfeldt and Gelhar* [1992], Figure 8 in *Garabedian et al.* [1991], and Figure 2 in *Linderfelt and Wilson* [1994] all show that the hydraulic gradient can vary significantly with time. Two of these plots are reproduced here as Figure 3.1.

The underlying cause of the gradient variability, as discussed in section 2, is variability in the regional boundary conditions. Therefore, it should be possible to estimate the variability in $J_i(t)$ from measurements of the boundary heads $H(\mathbf{x},t)$. In the case of an aquifer-connected lake, the boundary head is easy to measure and such measurements are generally reliable. For the purposes of this discussion, a hypothetical site is constructed with reasonable geometry and physical parameters. Figure 3.2 shows the physical attributes of the site, including the location of three imposed constant head boundaries. A lake boundary, ∂D_l, has been added to up-gradient and down-gradient head conditions, ∂D_u and ∂D_d. A no flux condition is imposed on the remainder of the boundary. Also shown in Figure 3.2 are nominal values for the three constant head boundaries. The ocean is assumed to be located at $x_1 = 10$ km, where the head is fixed at zero.

EXAMPLE 1: VARIABLE LAKE LEVEL

For the first example the upstream and downstream head boundaries are held constant while the lake level is allowed to vary. The lake rises and falls in time, possibly in response to surface runoff or stream inflow. It is assumed that the time series of lake level is known.

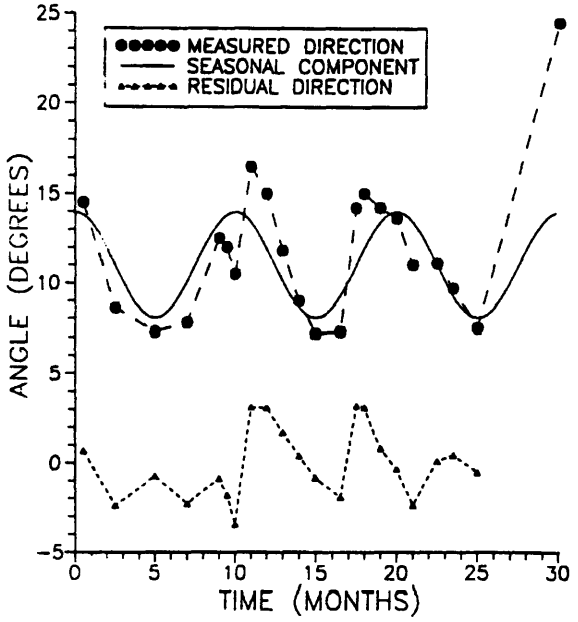

(a) From *Rehfeldt and Gelhar* [1992,Figure 2]. Cape Cod tracer test site. Note the seasonal periodicity, which the authors remove from the data.

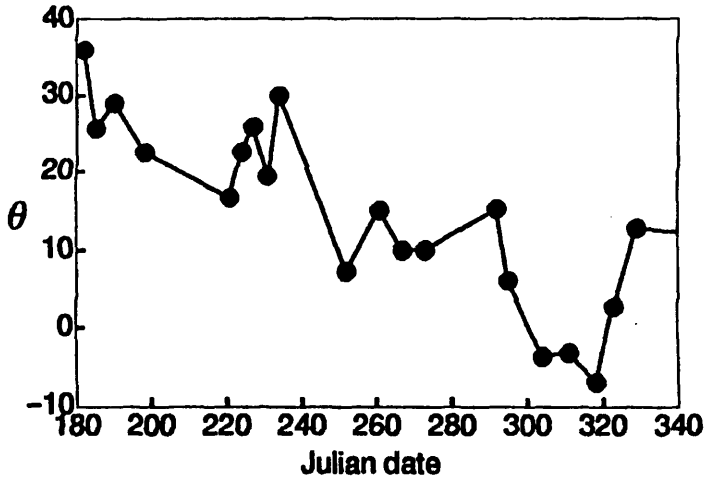

(b) From *Linderfelt and Wilson* [1994, Figure 2]. Site in Ontario, Canada.

Figure 3.1 Gradient direction time series measured at two groundwater study sites. Angles given in degrees.

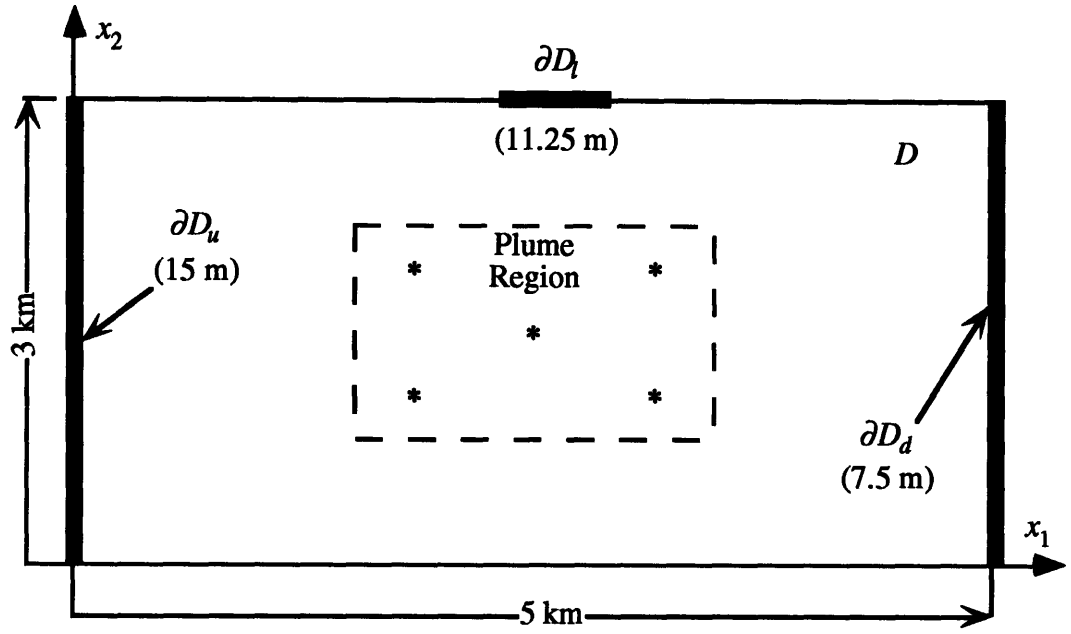

Figure 3.2 Site layout for Examples 1 and 2. The boundary head values correspond to the mean condition of Example 1. Hydraulic gradient components are recorded and averaged at the locations marked by an asterisk (*).

Because the lake is hydraulically connected to the aquifer (it is merely an expression of the water table), when its head is relatively low, water flows more toward the lake. In periods of high lake levels, water in the aquifer is pushed away from the lake. Thus, the gradient direction fluctuates in response to lake level changes.

To quantify this effect, a two-dimensional numerical flow model of the hypothetical site is used. The input conductivity field is uniform (representing the effective conductivity) and the nominal heads are imposed at the boundaries ∂D_u, ∂D_d, and ∂D_l. The simulated heads for this case are shown in Figure 3.3(a). The head in the lake is represented by H_l. For this example, it is assumed that the nominal head of 11.25 meters represents the long term average of the lake level, $\overline{H_l}$. Several flow simulations are conducted to model the effect of a range of lake levels around $\overline{H_l}$. For each simulation run, the output head field is stored for analysis (see Figure 3.3(b) and (c)).

For each modeled H_l, the head field is analyzed in the region marked "plume region" in Figure 3.1. Note that the plume region is far from the boundaries, satisfying the assumption made in Section 2. For a given H_l, the gradient doesn't vary much in the plume region (coefficient of variation generally under 15%), and a spatial average yields

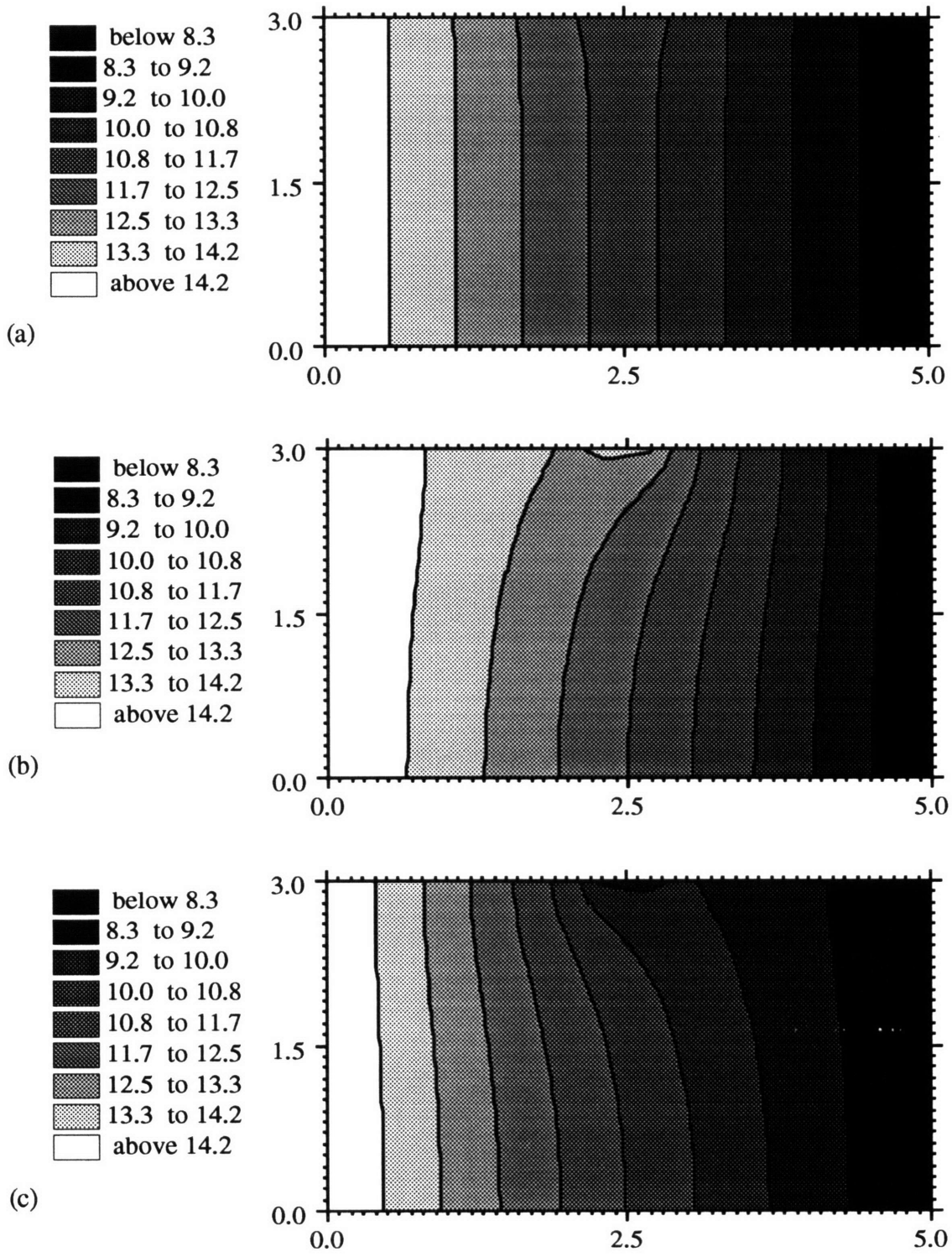

Figure 3.3 Head contours for Example 1. $H_u = 15$ m, $H_d = 7.5$ m. (a) Mean condition: $H_l = 11.25$ m. (b) High lake level: $H_l = 13.5$ m. (c) Low lake level: $H_l = 9.0$ m.

J_i for any time when the lake level is H_l (recall that aquifer storage is assumed to be negligible). Plots of J_1 and J_2 (Figure 3.4) reveal that each component is a linear function of H_l (thanks to our simple geometry and assumed isotropy) and can be written:

$$J_1(t) = c_1 + m_1 H_l(t); \quad J_2(t) = c_2 + m_2 H_l(t) \tag{3.1}$$

with means and perturbations given by:

$$\overline{J_1} = c_1 + m_1 \overline{H_l}; \quad \overline{J_2} = c_2 + m_2 \overline{H_l} \tag{3.2}$$

$$J'_{b1}(t) = m_1 H'_l(t); \quad J'_{b2}(t) = m_2 H'_l(t) \tag{3.3}$$

For this special case (with the mean lake level equal to the average of the imposed upstream and downstream heads, and with the lake and plume region centered at $x_1 = 2.5$ km), m_1 , J'_{b1}, and $\overline{J_2}$ are zero, and the mean gradient is in the x_1 direction:

$$\overline{J_1} = c_1 = J \tag{3.4}$$

taking the slope of Figure 3.4(b) for m_2, the transverse gradient auto-covariance is represented by

$$R_{J_2 J_2}(t_2 - t_1) = \overline{J'_{b2}(t_1) J'_{b2}(t_2)} = (m_2)^2 \overline{H'_l(t_1) H'_l(t_2)} = (m_2)^2 R_{H_l H_l}(t_2 - t_1) \tag{3.5}$$

and Fourier transforming the covariance functions gives the gradient spectrum in terms of the lake level spectrum:

$$S_{J_2 J_2}(\omega) = (m_2)^2 S_{H_l H_l}(\omega) \tag{3.6}$$

In this case the J'_{b1} auto-spectrum and the gradient cross-spectra are zero.

EXAMPLE 2: VARIABLE UPGRADIENT RECHARGE

To model the effect of variable inflow from an upgradient recharge zone, the lake level is held constant while upstream and downstream heads are varied. Since, for the hypothetical site, the ocean is located at $x_1 = 10$ km, the downgradient head is always prescribed to be half of the upstream head (this assumes that the aquifer material is similar downgradient of the site). Neglecting flow in and out of the lake, the upgradient recharge rate, Q [L^3/T], is roughly described by

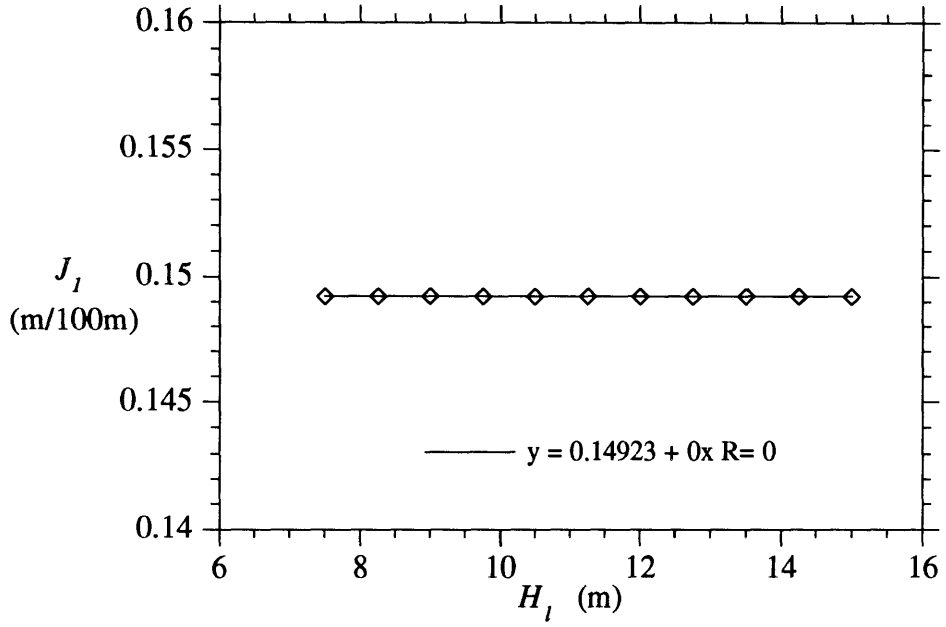

(a) Longitudinal gradient as a function of lake level.

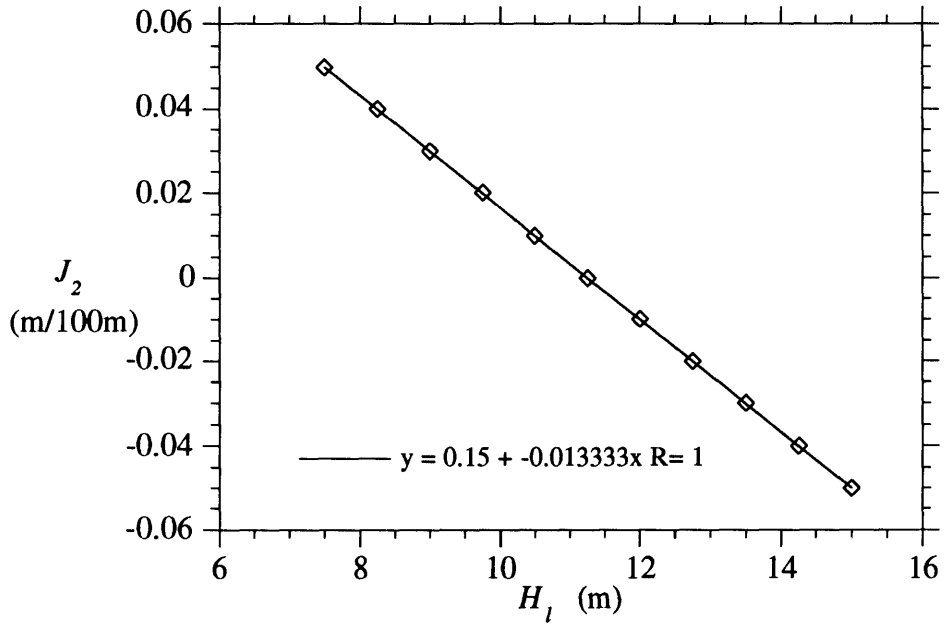

(b) Transverse gradient as a function of lake level.

Figure 3.4 Gradient components as a function of lake level for Example 1.

$$Q = \hat{K}\frac{\Delta H}{l}(wd) \propto H_u \tag{3.7}$$

where $\hat{K}$ is the effective conductivity, ΔH is the difference between upgradient and downgradient heads, l, w, and d are the regional site dimensions, and H_u is the prescribed upgradient head. For this example, the mean value of H_u is taken to be 15 m, and the lake level is fixed at 10 m. Flow simulations are conducted for H_u values ranging from 10 to 20 meters (with downstream heads ranging from 5 to 10 m), and a spatially averaged J_i is determined for the plume region. Figure 3.5 shows some contour plots of the head data for this example.

As in Example 1, the plots of J_i versus the boundary head (in this case H_u) are linear (see Figure 3.6) and equations (3.2) and (3.3) apply. However, the unique symmetry of Example 1 does not apply in this case because at the mean condition the lake level is less than the average of the two boundary heads and the gradient is angled slightly from horizontal. In this case, m_1 , J_1', and $\overline{J_2}$ are all non-zero. To aid analysis, the coordinate system is rotated by an angle θ to the regional axes, where

$$\theta = \tan^{-1}\left(\overline{J_2}/\overline{J_1}\right) \tag{3.8}$$

so that in the rotated coordinate system (see Figure 3.7) the mean gradient is in the x_1 direction. In rotated coordinates hydraulic gradient, as a function of upgradient head, is

$$J_1^R = c_1^R + m_1^R H_u; \quad J_2^R = c_2^R + m_2^R H_u \tag{3.9}$$

with rotations performed in the usual way:

$$\begin{aligned} c_1^R &= c_1\cos\theta + c_2\sin\theta; \quad m_1^R = m_1\cos\theta + m_2\sin\theta \\ c_2^R &= c_2\cos\theta - c_1\sin\theta; \quad m_2^R = m_2\cos\theta - m_1\sin\theta \end{aligned} \tag{3.10}$$

With this coordinate rotation, it can be confirmed that

$$J_1^R\left(\overline{H_u}\right) = \sqrt{\overline{J_1}^2 + \overline{J_2}^2} = J \tag{3.11}$$

and

$$J_2^R\left(\overline{H_u}\right) = 0 \tag{3.10}$$

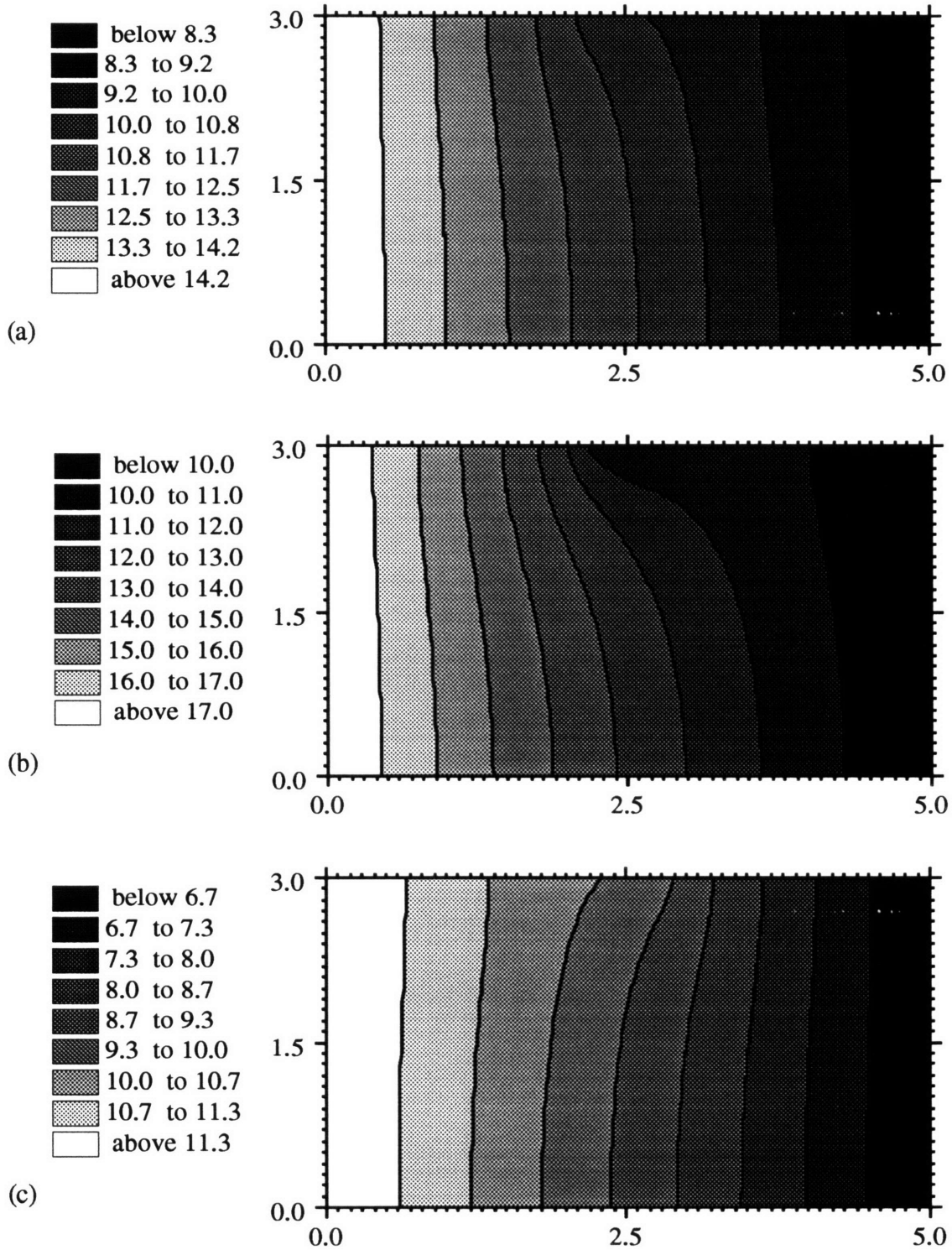

Figure 3.5 Head contours for Example 2. $H_d = 7.5$ m, $H_l = 10$ m. (a) Mean condition: $H_u = 15$ m. (b) High upgradient head: $H_u = 18$ m. (c) Low upgradient head: $H_u = 12$ m.

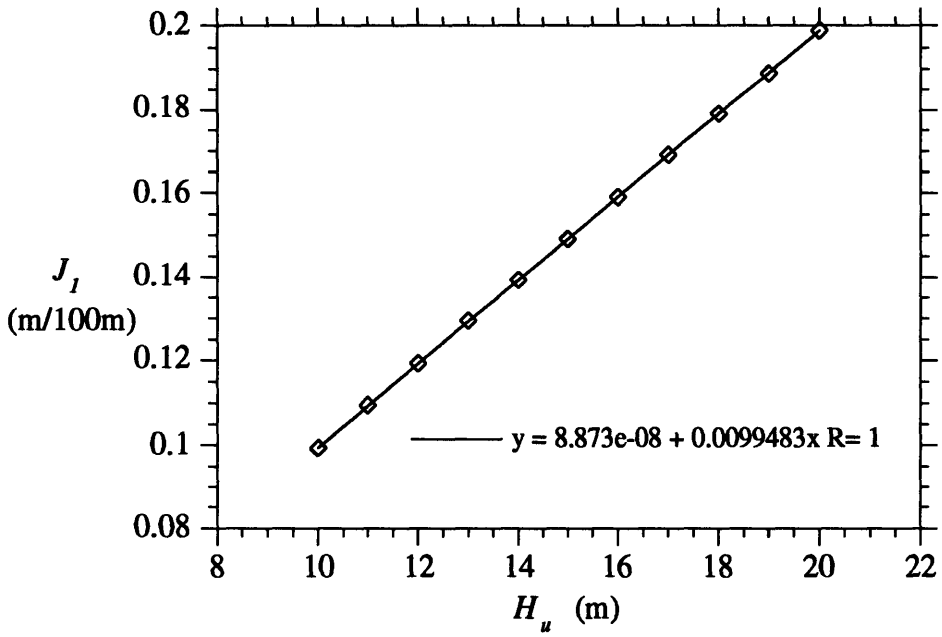

(a) Longitudinal gradient as a function of upgradient head.

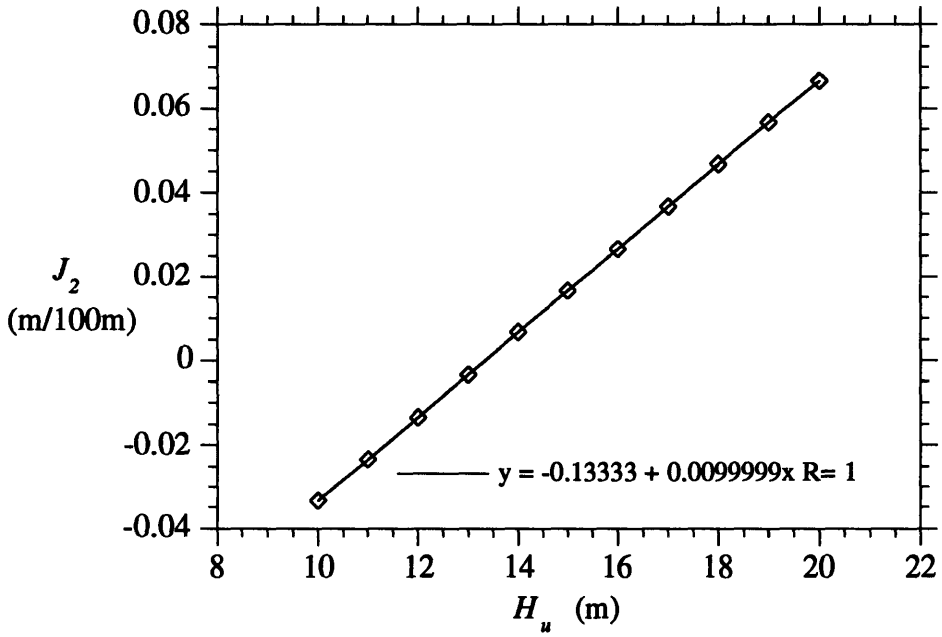

(b) Transverse gradient as a function of upgradient head.

Figure 3.6 Gradient components as a function of upgradient head for Example 2.

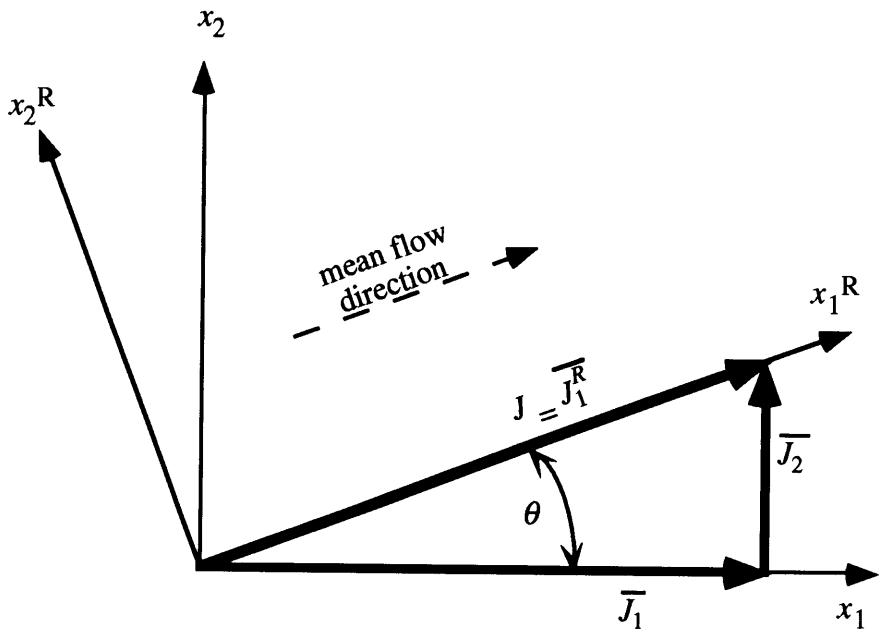

Figure 3.7 Mean gradient rotation.

Using the rotated coordinates and slope parameters, but dropping the R superscripts, the following spectral relationships hold:

$$S_{J_1J_1}(\omega) = (m_1)^2 S_{H_uH_u}(\omega) \tag{3.11a}$$

$$S_{J_2J_2}(\omega) = (m_2)^2 S_{H_uH_u}(\omega) \tag{3.11b}$$

$$S_{J_1J_2}(\omega) = S_{J_2J_1}(\omega) = m_1 m_2 S_{H_uH_u}(\omega) \tag{3.11c}$$

Note that if the recharge, Q, had been used throughout as the measure of boundary variability, expressions similar to (3.11) would result with $S_{H_uH_u}(\omega)$ replaced by $S_{QQ}(\omega)$.

DISCUSSION

This section suggests a logical procedure for determining the macrodispersivity and modeling a real contamination plume, based solely on information about the hydraulic conductivity and regional flow boundaries. Namely, the following steps would be taken:

- Sample the site for hydraulic conductivity; estimate the log-conductivity mean and variance as well as the correlation structure. (Alternatively, infer the conductivity statistics from measurements at geologically similar sites.)

- Collect information on regional hydraulic controls of the aquifer (e.g. lake levels, recharge rates).
- Model groundwater flow at the regional scale.
- Following the procedure described in Examples 1 and 2 above, estimate the direction of mean flow, the magnitude of the mean gradient, and the gradient sensitivity parameters, m_i.
- Estimate the effective conductivity and mean velocity from (2.54) and (2.51).
- Perform a spectral analysis of the regional boundary data (see example in Appendix C).
- Using the estimated boundary spectral density functions and the slope parameters, m_i, compute $S_{J_i J_j}(\omega)$ at discrete frequencies.
- Numerically integrate (2.60) with the estimated spectra to obtain values for $A_{ij}^{(st)}$.
- Use *Gelhar and Axness* [1983] and *Rehfeldt and Gelhar* [1992] to determine $A_{ij}^{(s)}$ and $A_{ij}^{(t)}$.
- Use the total macrodispersivity to model the large-time behavior of a conservative solute, according to (2.11).

This exercise could theoretically be applied in the field to produce estimates for macrodispersivity. The estimates could be verified using concentration data at a study site. However, this thesis stops short of applying the theory at a field site. Instead, in the next section we use a model boundary head spectrum and physically realistic parameters to study when the effect of the new term, $A_{ij}^{(st)}$, is important in the prediction of total macrodispersivity. In order to apply the methods described above in the field, it is necessary to have a good understanding of the regional flow controls and a long time record of boundary conditions (e.g. lake levels, see Appendix C).

4. APPLICATION

The stochastic development in Section 2 leads to a macrodispersivity expression (2.50) that can be written as the sum of three terms:

1) $A_{ij}^{(s)}$, the *Gelhar and Axness* [1983] macrodispersivity due to aquifer heterogeneity;

2) $A_{ij}^{(t)}$, the *Rehfeldt and Gelhar* [1992] macrodispersivity due to a variable hydraulic gradient; and

3) $A_{ij}^{(st)}$, a new term that represents the additional, combined effect of aquifer heterogeneity and gradient variability.

In this section we examine the relative importance of these terms, and how the magnitude of each changes under different geologic and hydrologic conditions. Sections 2 and 3 show that the total macrodispersivity will depend on the spatial statistics of hydraulic conductivity at the site, the temporal statistics of the flow boundaries, and the sensitivity of the plume-area gradient to fluctuations in the boundary conditions. To quantify the approximate macrodispersivity and to get a feel for when the third term, $A_{ij}^{(st)}$, becomes important, we examine a nominal case, with given physical parameters, and observe how the results change for different parameter values.

NOMINAL CASE

We begin our examination by considering nominal, physically plausible aquifer conditions that are within the range typically observed at field sites. After listing the nominal inputs, we calculate the macrodispersivity using the theories of *Gelhar and Axness* [1983], *Rehfeldt and Gelhar* [1992], and this thesis.

Inputs for the Nominal Case

The parameter values chosen for the nominal case are listed in Table 4.1. These values are reasonable for a heterogeneous site where the gradient is highly variable. This type of site is common, and illustrates the usefulness of the $A_{ij}^{(st)}$ term.

Table 4.1 Nominal Parameters

Parameter	*Value*
K_g	4.1 m/day
σ_f	1.0
λ_f	3.0 m
n	0.30
J	0.01
q	0.03 m/day*
v	0.1 m/day*
a_H	0.5 m
ω_0	0.0172 rad/day
σ_H	0.2 m
λ_H	30 days
m_1	0.01 m^{-1}
m_2	0.01 m^{-1}

*derived from the other parameters

For this study, consider a variable aquifer-connected lake like the one in Example 1 of Section 3. This lake controls the direction and magnitude of the hydraulic gradient at a distant plume region (note that the symmetry of Example 1 is not assumed here). The lake responds to storm events and varies as the climate undergoes seasonal changes. The level of the lake on a given day is expected to be well-correlated with the lake level on the previous day, and also somewhat correlated with the lake level one year beforehand. Thus the spectrum of the lake level will have a significant peak at a frequency corresponding to the 1-year cycle (see Appendix C). The third term in the macrodispersivity expression (2.50) is believed to be significant when there is high-frequency energy in the spectrum.

To determine when high-frequency variations become significant, a generic boundary head spectrum is introduced. This model spectrum has the following form:

$$S_{HH}(\omega) = \frac{\sigma_H^2 \lambda_H}{\pi\left(1+\lambda_H^2\omega^2\right)} + \frac{a_H^2}{4}\delta(\omega \pm \omega_0) \tag{4.1}$$

and is depicted graphically in Figure 4.1. The first term in this spectrum is that for a Markov process with variance σ_H^2 and correlation time scale λ_H. In a Markov process, the correlation between two head measurements decreases exponentially as the measurement spacing increases. Superimposed on this spectrum is a delta function, representing a perfect harmonic process with amplitude a_H and frequency ω_0. For the nominal case, the periodic component of the lake fluctuates with a period of one year (characteristic frequency, ω_0, of 0.0172 radians per day) and an amplitude, a_H, of 0.5 meters. The Markovian component has a standard deviation, σ_H, of 0.2 meters and a correlation scale, λ_H, of 30 days.

The log-conductivity, f, is assumed to be isotropic and well-described by an exponential covariance. Thus the log-conductivity spectrum is

$$S_{ff}(k) = \frac{\sigma_f^2 \lambda_f^3}{\pi^2\left(1+\lambda_f^2 k^2\right)^2} \tag{4.2}$$

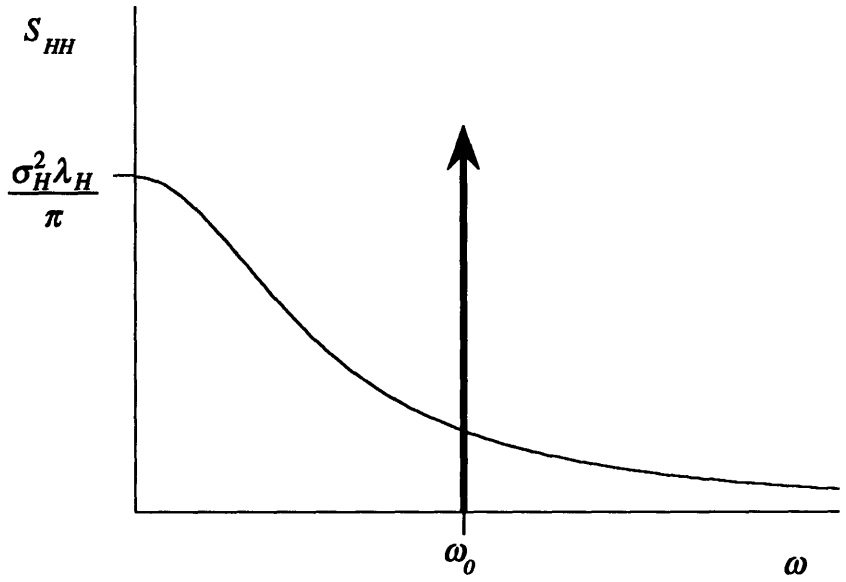

Figure 4.1 Shape of the model boundary head spectrum.

For the nominal case, the log-conductivity length scale, λ_f is taken to be 3.0 meters, and the standard deviation, σ_f is 1.0. The geometric mean hydraulic conductivity, K_g is taken to be 4.1 meters per day, and the porosity is 30%.

The boundary-determined mean hydraulic gradient, J, has a value of 0.01 for this study, giving a mean specific discharge, q, of 0.03 meters per day, and a pore velocity, v, of 0.1 meters per day.

The sensitivities of the gradient components to the boundary head fluctuations are given by the modeled slope parameters, m_1 and m_2. In the nominal case, each of these parameters is assigned a value of 0.01 per meter. So in the nominal case, if the lake level is 0.1 meter above its average, then the gradient components are 0.011 and 0.001 respectively (the gradient is at an angle of 5.2° from its mean direction). Note that in our nominal case, the gradient variability is large. If the peak lake level is approximately 0.7 meters (amplitude plus one standard deviation) above its mean, then the maximum longitudinal and transverse gradient components are 0.017 and 0.007 respectively.

Since we are looking for macrodispersivity values that are much larger than local dispersivity (which is usually on the order of millimeters), we assume that the local dispersivity is zero.

Macrodispersivity From Heterogeneity Only

Gelhar and Axness presented results for macrodispersivity in a three-dimensional isotropic medium with a steady gradient. Their results (equations 33 and 37) are restated here:

$$A_{ij}^{(s)} = 0; \quad i \neq j \tag{4.3}$$

$$A_{11}^{(s)} \cong \frac{\sigma_f^2 \lambda_f}{\gamma^2} \tag{4.4}$$

$$A_{22}^{(s)}, A_{33}^{(s)} \propto \text{local dispersivity} \cong 0 \tag{4.5}$$

The *Gelhar and Axness* expression for steady longitudinal dispersivity (4.4) is accepted as a good order-of-magnitude approximator. However, observed horizontal transverse dispersivities are often at least an order of magnitude higher than the *Gelhar and Axness* transverse dispersivity prediction.

For our nominal case, the steady longitudinal dispersivity is 2.2 meters. This value increases as the conductivity length scale and the log-conductivity variance increase.

Macrodispersivity From Gradient Variability Only

Rehfeldt and Gelhar extended the steady analysis to include the first-order effect of a random gradient. Their total macrodispersivity was the sum of $A_{ij}^{(s)}$ and $A_{ij}^{(t)}$. The solution for $A_{ij}^{(t)}$ was shown to be proportional to the power of the gradient spectrum at zero frequency and independent of aquifer heterogeneity. Thus, periodicity in the gradient had no effect on dispersivity in the *Rehfeldt and Gelhar* analysis. Their result for a Markov J process in isotropic media is given by

$$A_{ij}^{(t)} = \frac{v}{\gamma^2}\frac{\sigma_{J_iJ_j}^2}{J^2}\lambda_J \tag{4.6}$$

where the gradient variance is the boundary induced variability, equivalent to the gradient spectrum responses derived in Section 3:

$$\sigma_{J_iJ_j}^2 = m_i m_j \sigma_H^2;\ \ \lambda_J = \lambda_H \tag{4.7}$$

For the nominal case, the $A_{ij}^{(t)}$ components are:

$$\begin{gathered} A_{11}^{(t)} = A_{22}^{(t)} = A_{12}^{(t)} = A_{21}^{(t)} = 0.089 \text{ m} \\ \text{all other } A_{ij}^{(t)} = 0 \end{gathered} \tag{4.8}$$

Note that this term will not add much to the longitudinal macrodispersivity, but it is much larger than local dispersivity, and so it will be important for the transverse and off-diagonal (plume-rotation) terms. When the boundary process has no periodicity, we expect this term to dominate the transverse dispersivity expression. For our nominal case, $A_{22}^{(t)}$ is about 4% of $A_{11}^{(s)}$. This estimate is sensitive to the Markovian boundary variance and correlation time. The predicted value of $A_{ij}^{(t)}$ increases linearly with groundwater velocity. This term does not depend on the aquifer heterogeneity (except, possibly in a minor way via the flow factor, γ).

Macrodispersivity From the Combination of Gradient Variability and Heterogeneity

The last macrodispersivity term, $A_{ij}^{(st)}$, is new with this thesis, and includes the effect of heterogeneity *and* gradient variability. The evaluation of the integral expression (2.60) for harmonic, Markov, and combined spectra is carried out in Appendix D. The results are complicated functions of many variables and can best be shown graphically. We are especially interested in situations when any component of the $A_{ij}^{(st)}$ tensor adds a significant amount to the total macrodispersivity, A_{ij}.

Using the nominal conditions and the equations in Appendix D, the third macrodispersivity term has components:

$$\begin{aligned} A_{11}^{(st)} &= 0.18 \text{ m} \\ A_{22}^{(st)} &= 0.14 \text{ m} \\ A_{33}^{(st)} &= 0.037 \text{ m} \\ A_{12}^{(st)} &= A_{21}^{(st)} = 0.13 \text{ m} \\ A_{13}^{(st)} &= A_{31}^{(st)} = A_{23}^{(st)} = A_{32}^{(st)} = 0 \end{aligned} \tag{4.9}$$

which gives total macrodispersivities of:

$$\begin{aligned} A_{11} &= 2.47 \text{ m} \\ A_{22} &= 0.23 \text{ m} \\ A_{33} &= 0.037 \text{ m} \\ A_{12} &= A_{21} = 0.22 \text{ m} \\ A_{13} &= A_{31} = A_{23} = A_{32} = 0 \end{aligned} \tag{4.10}$$

The off-diagonal terms A_{12} and A_{21} cause plume rotation. In the x_i coordinate system that is aligned with the mean flow direction, the non-zero off-diagonal terms imply that a mean concentration gradient in the longitudinal direction creates a dispersive flux in the transverse, and vice-versa. Following *Bear* [1972, p.139-140], rotating to a coordinate system x_i' by an angle η given by

$$\eta = \frac{1}{2}\tan^{-1}\left(\frac{A_{12}}{A_{11} - A_{22}}\right) \tag{4.11}$$

results in a diagonalized matrix with components

$$\begin{aligned} A'_{11} &= \frac{A_{11}+A_{22}}{2} + \frac{A_{11}-A_{22}}{2}\cos 2\eta + K_{12}\sin 2\eta \\ A'_{11} &= \frac{A_{11}+A_{22}}{2} - \frac{A_{11}-A_{22}}{2}\cos 2\eta - K_{12}\sin 2\eta \\ A'_{12} &= A'_{21} = 0 \end{aligned} \tag{4.12}$$

(the other terms are unaffected). For the nominal case, the plume is rotated by a small angle, $\eta = 2.9°$, and the diagonalized longitudinal and transverse components are not much different from the original ones:

$$\begin{aligned} A'_{11} &= 2.49 \text{ m} \\ A'_{22} &= 0.22 \text{ m} \end{aligned} \tag{4.13}$$

The nominal case shows that the third term in the total dispersivity equation can have a significant effect on the transverse dispersivity estimates. The nominal case results agree with the rule of thumb that the field dispersivities are roughly in the ratio:

$$A_{33} : A_{22} : A_{11} = 1:10:100 \tag{4.14}$$

Of course, the magnitude of $A_{ij}^{(st)}$ and the total dispersivities would be different if other parameters were used in the expressions; this case just points out that the $A_{ij}^{(st)}$ term can be large for a particular, physically reasonable, set of parameters.

OTHER AQUIFER CONDITIONS

We now generalize our study, examining the conditions when each of the incrementally different theories (*Gelhar and Axness*, *Rehfeldt and Gelhar*, and this thesis) are appropriate. We begin by studying the sensitivity of the three theoretical estimates to departures from the nominal case, and then draw conclusions about the applicability of each of the theories to any given site.

Departures from the Nominal Case

To see how the values of $A_{ij}^{(st)}$ and the total dispersivity change when the site parameters are different, we examine departures from the nominal case, one variable at a time. Figures 4.2–4.7 (included at the end of this section) each show the

macrodispersivity value as a function of one of the site parameters (the other parameters are held at the nominal values). Each figure has four plots, one for each diagonal component of the macrodispersivity tensor and one for the horizontal rotation components. Each of the four plots contains three lines, corresponding to the total dispersivity predicted in 1) *Gelhar and Axness* [1983], 2) *Rehfeldt and Gelhar* [1992], and 3) this thesis.

Figure 4.2 points out the importance of the periodic component of the spectrum. If the lake amplitude is large (causing a large periodic change in the gradient), then the total dispersivities are increased significantly, and the $A_{ij}^{(st)}$ terms are important. If there is no periodicity in the lake level, and the Markov process dominates, then the *Rehfeldt and Gelhar* approximations are good. Figure 4.3 shows that the third term is a marginal improvement to the *Rehfeldt and Gelhar* approximation when the Markovian component of the boundary spectrum is large compared to the periodic component.

Figures 4.4 and 4.5 demonstrate the importance of the parameters m_1 and m_2, which measure the sensitivity of the gradient components to the boundary fluctuations. When m_1 is large, the A_{11} term is most affected, and when m_2 is large, A_{22} is most affected. In each case, when m_i is high (indicating greater gradient variability compared to the mean), the $A_{ij}^{(st)}$ terms are important. Figure 4.6 demonstrates a similar effect: as the mean gradient magnitude increases, the effect of the variations becomes less important, and the *Gelhar and Axness* approximations become sufficient.

Finally, Figure 4.7 shows the effect of the geometric mean conductivity on the macrodispersivity. Highly conductive aquifers with gradient variability will exhibit greater macrodispersivities. The *Rehfeldt and Gelhar* approximations become more satisfactory at high conductivity.

In all of Figures 4.2-4.7, the off-diagonal term A_{12} can be significant for certain parameter values. Thus, it is possible for the plume to be at a significant angle to the flow axis, and the diagonalized dispersivity values could differ significantly from the non-rotated dispersivities.

General Applicability of the Different Macrodispersivity Estimates

It is difficult to show with precision which theory is sufficient under general aquifer conditions. However, the sensitivity analysis of the nominal case and the mathematical expressions of Section 2 have important implications.

In all of the Figures 4.2-4.7, the $A_{ij}^{(st)}$ term is significant when the variability of flow is large compared to the mean. Note also that the nominal case uses a standard deviation of one order of magnitude for the hydraulic conductivity. Large variability in the log-conductivity and hydraulic gradient lead to high energy spectra, and the product of the two spectra, appearing in the definition of $A_{ij}^{(st)}$, (2.50), is significant. Recall that this term arises because the product of the hydraulic gradient fluctuations and log-conductivity fluctuations is retained in the Darcy perturbation equation (2.31).

In cases where the gradient is highly variable, mean groundwater velocities are modest, and heterogeneity is significant, the third macrodispersivity term, $A_{ij}^{(st)}$ should be used to get a more accurate estimate of macrodispersivity. This term also incorporates the macrodispersive effects from a periodically varying gradient. If the gradient is not varying much, the *Gelhar and Axness* steady approximations are sufficient. For highly conductive aquifers with only modest periodicity in the gradient, the *Rehfeldt and Gelhar* theory provides a good approximation.

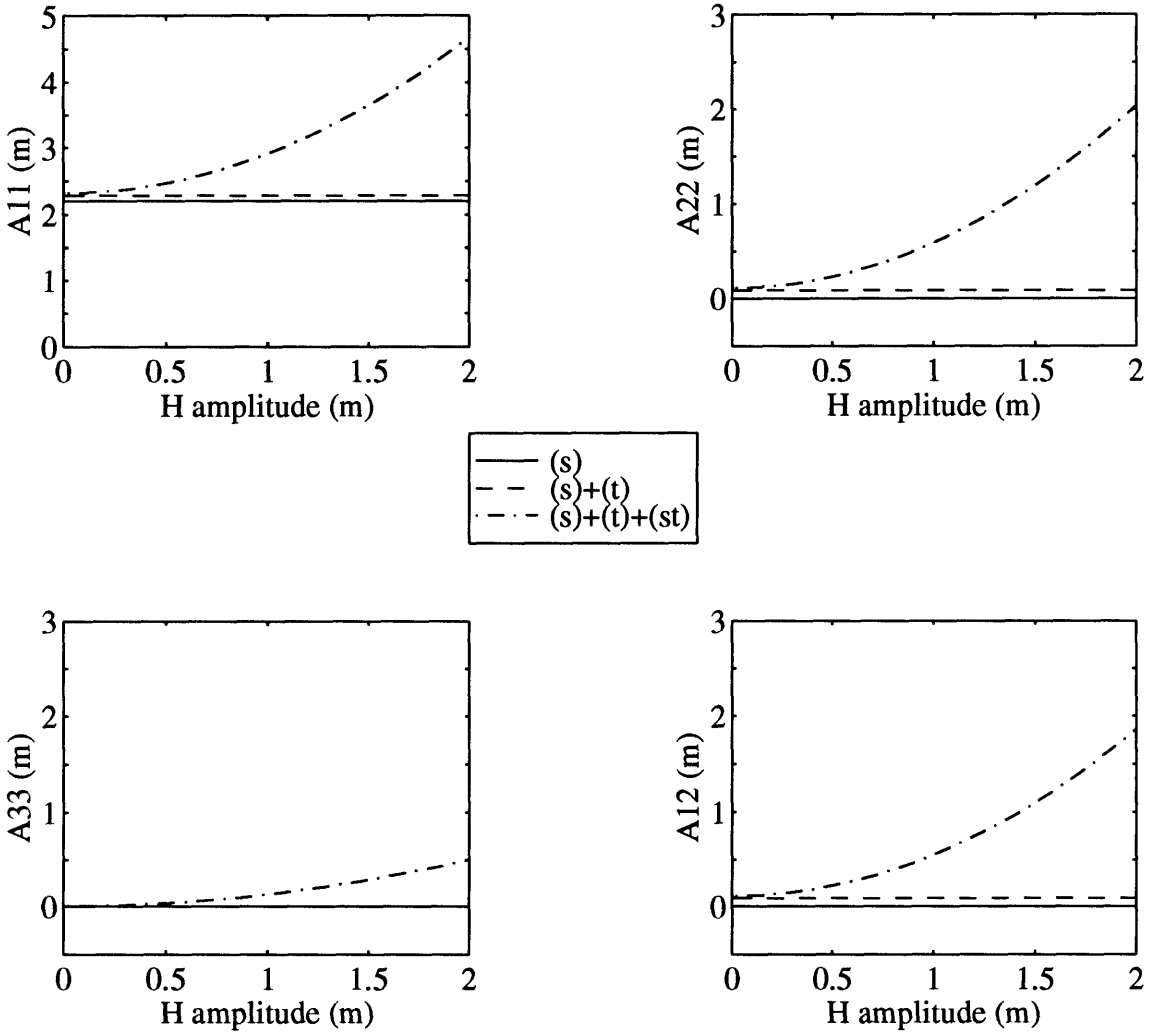

Figure 4.2 Macrodispersivity as a function of the boundary lake amplitude (a_H). Solid–*Gelhar and Axness*, Dashed–*Rehfeldt and Gelhar*, Dot-dashed–this thesis.

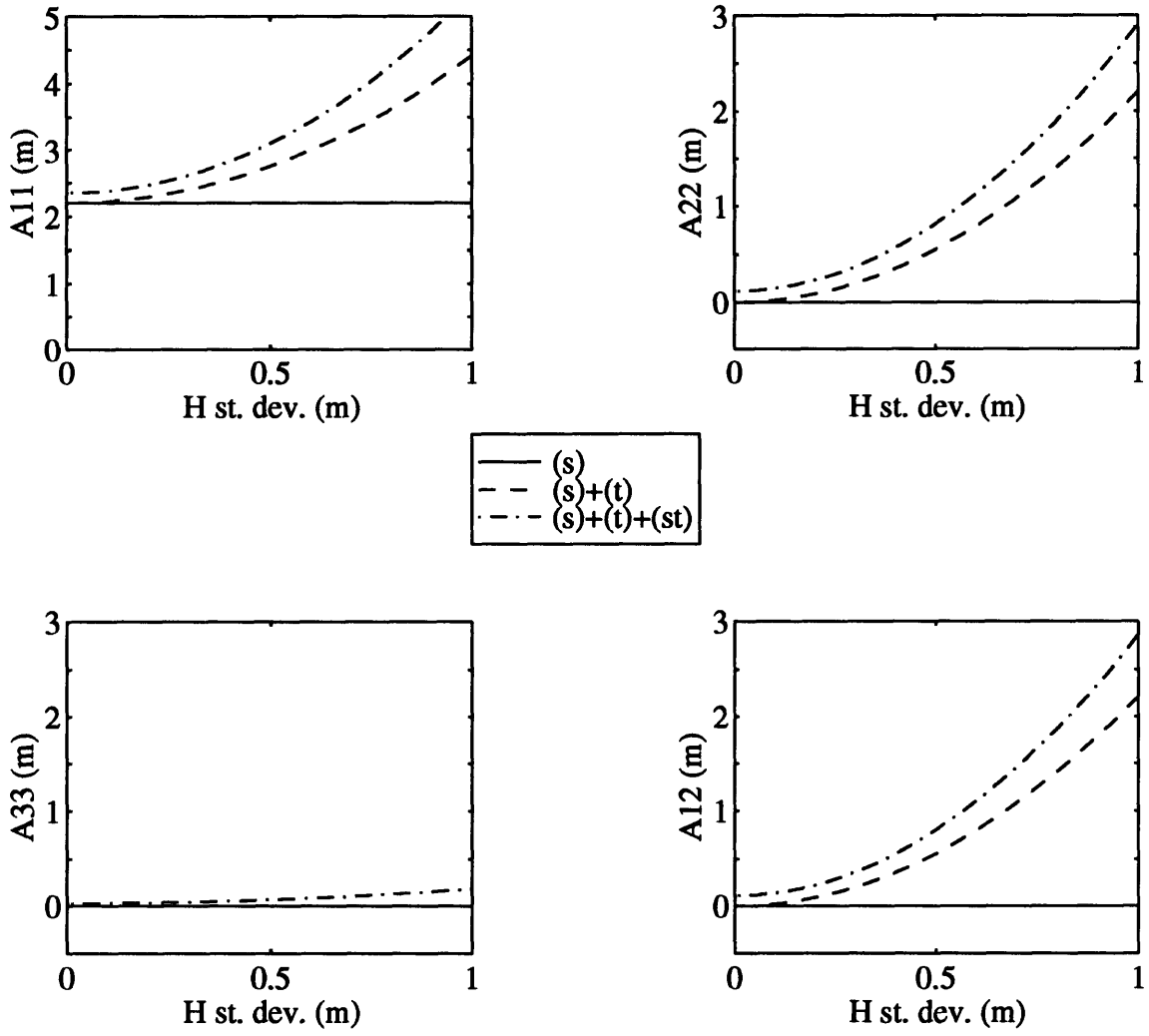

Figure 4.3 Macrodispersivity as a function of the boundary lake Markovian standard deviation (σ_H). Solid–*Gelhar and Axness*, Dashed–*Rehfeldt and Gelhar*, Dot-dashed–this thesis.

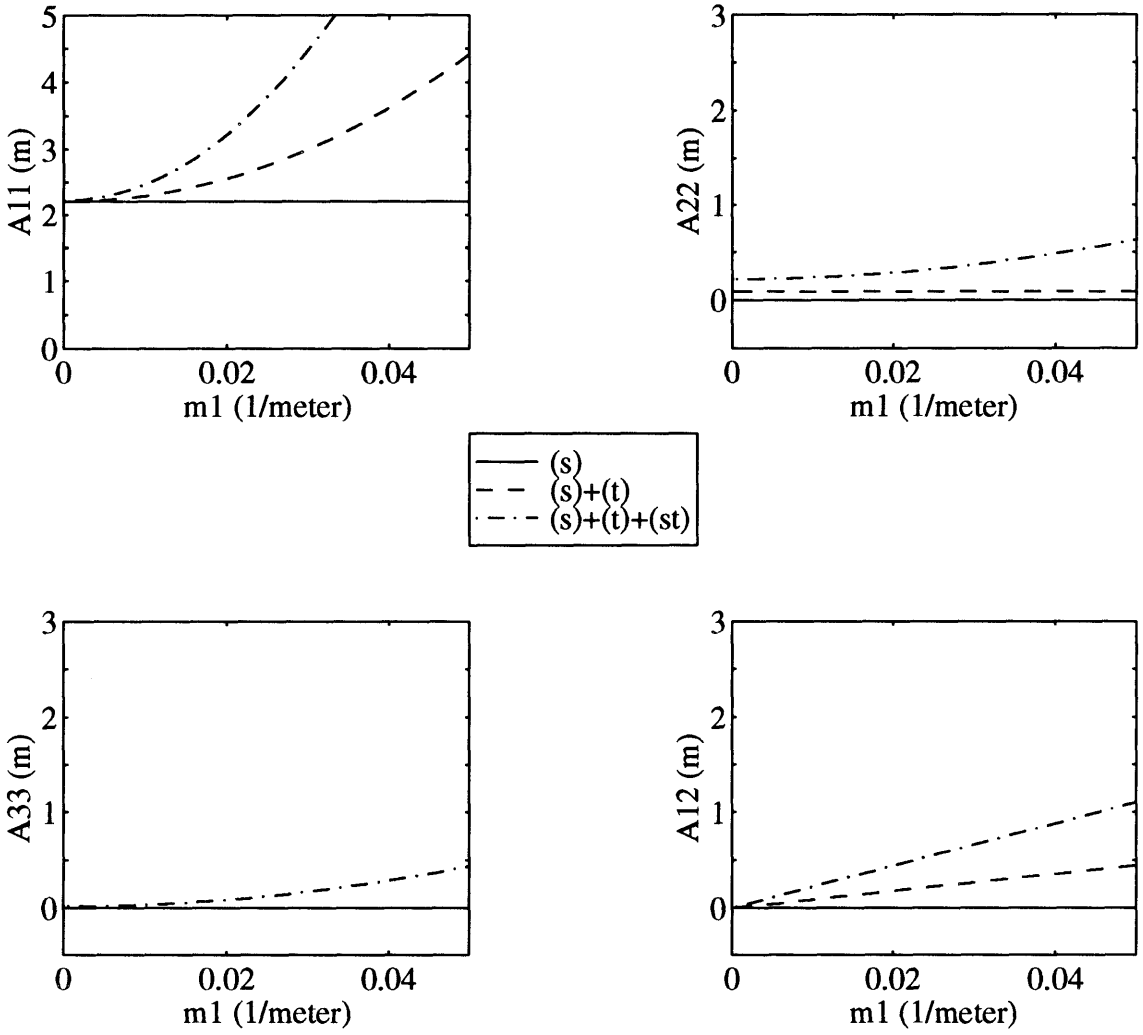

Figure 4.4 Macrodispersivity as a function of the longitudinal gradient sensitivity parameter, m_1. Solid–*Gelhar and Axness*, Dashed–*Rehfeldt and Gelhar*, Dot-dashed–this thesis.

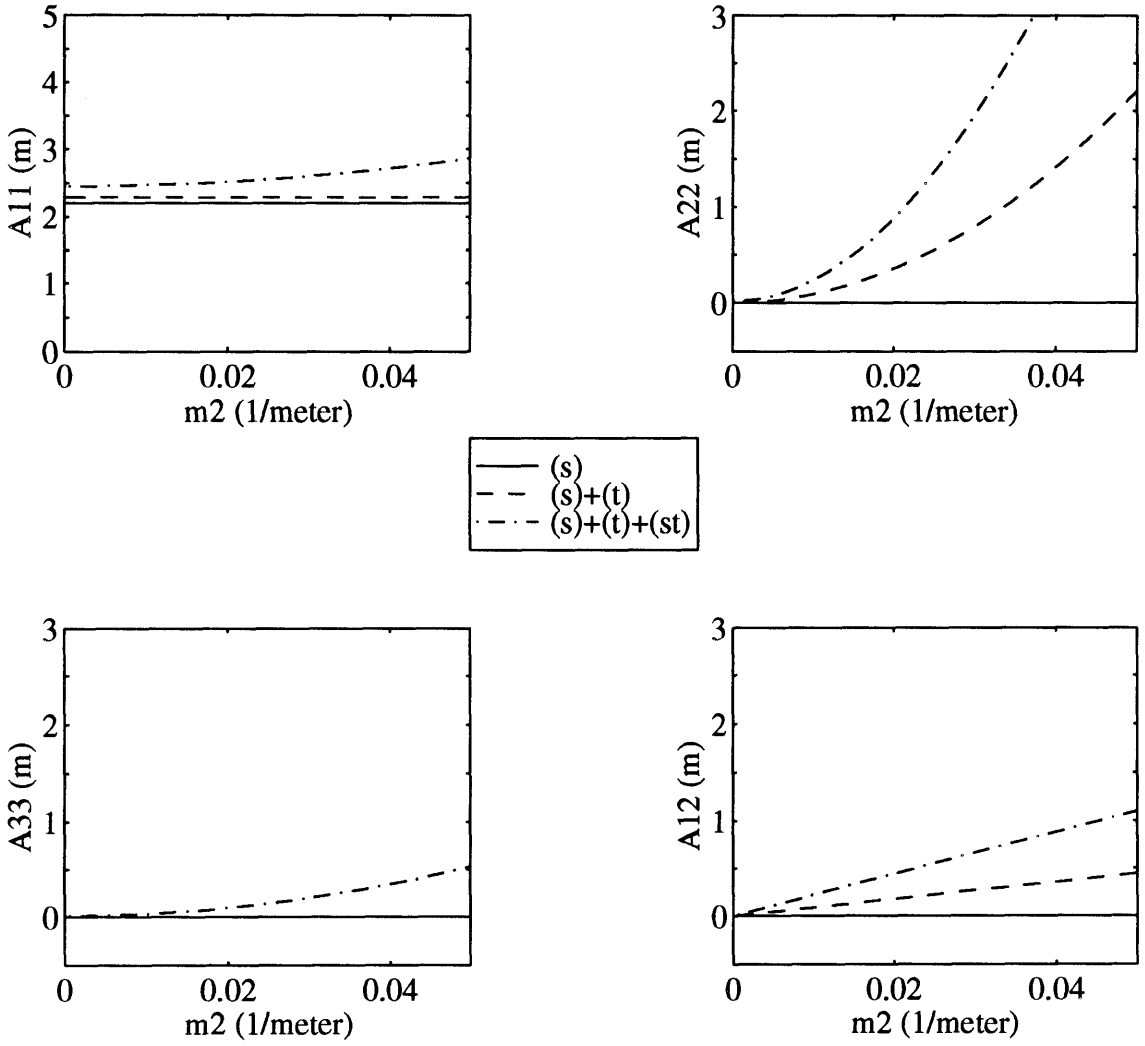

Figure 4.5 Macrodispersivity as a function of the transverse gradient sensitivity parameter, m_2. Solid–*Gelhar and Axness*, Dashed–*Rehfeldt and Gelhar*, Dot-dashed–this thesis.

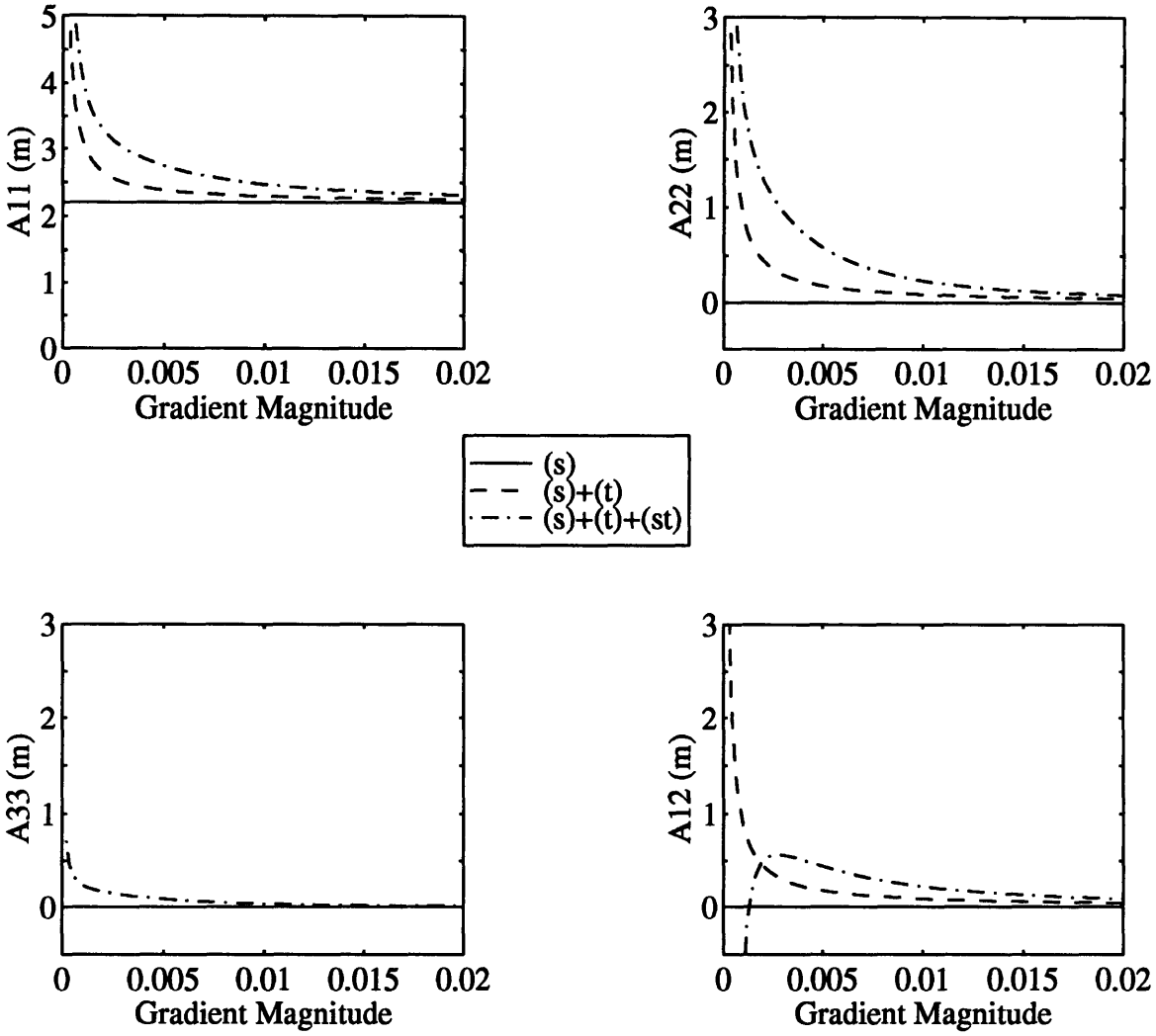

Figure 4.6 Macrodispersivity as a function of the mean hydraulic gradient magnitude (J). Solid–*Gelhar and Axness*, Dashed–*Rehfeldt and Gelhar*, Dot-dashed–this thesis.

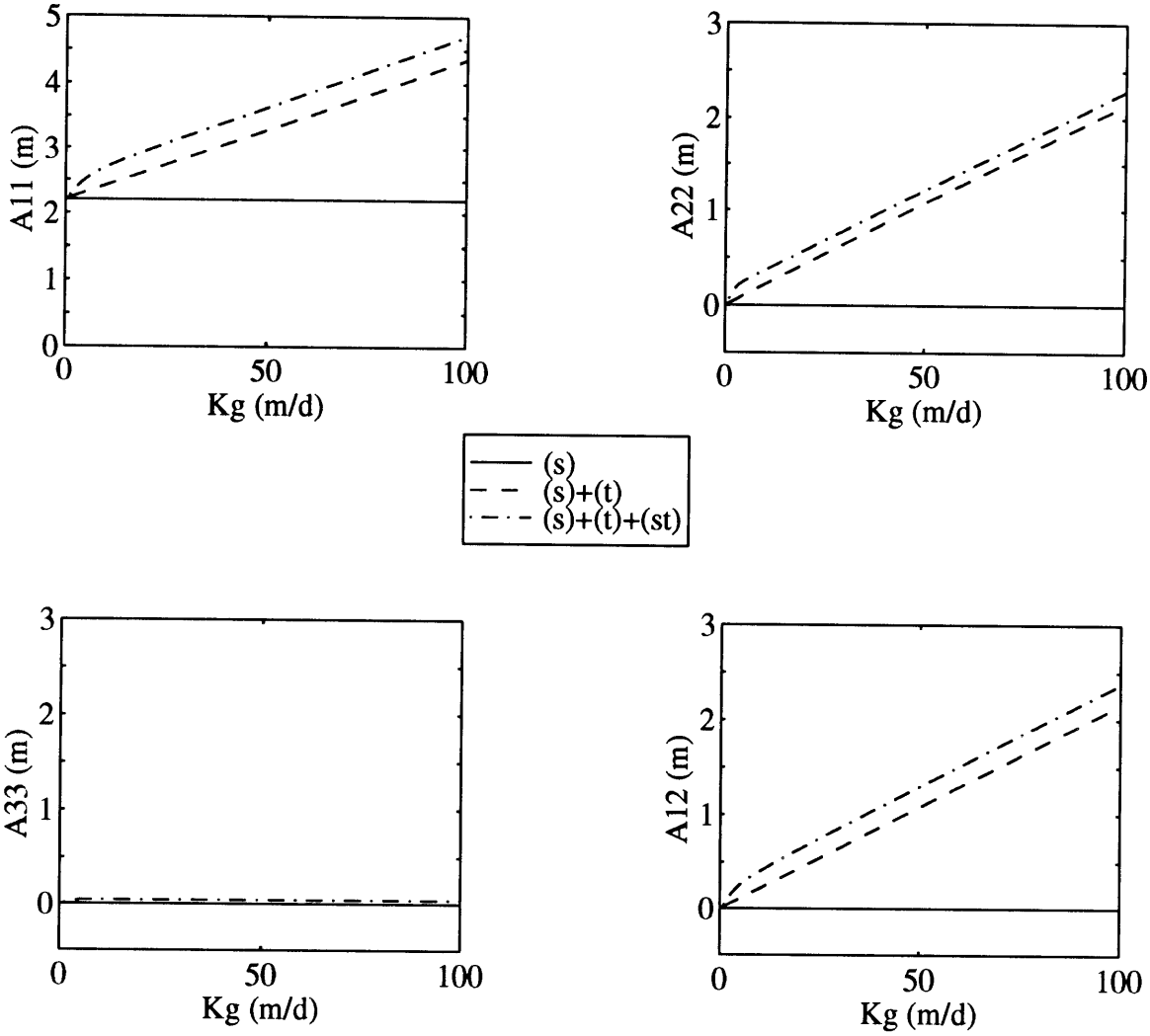

Figure 4.7 Macrodispersivity as a function of the geometric mean hydraulic conductivity (K_g). Solid–*Gelhar and Axness*, Dashed–*Rehfeldt and Gelhar*, Dot-dashed–this thesis.

5. CONCLUSIONS

For a given field site, the observed horizontal transverse dispersivity is generally around one order of magnitude smaller than the longitudinal dispersivity (with vertical dispersivity generally another order of magnitude smaller). The *Gelhar and Axness* [1983] approximation has proven to be an accurate estimate of the field longitudinal dispersivity, but the theory tends to underestimate the horizontal transverse dispersivity (at least when isotropy is assumed). With the *Rehfeldt and Gelhar* [1992] term added (and a gradient spectrum postulated), transverse macrodispersivity estimates come closer to those measured with moment analyses of tracer tests. Still, the approximations in *Rehfeldt and Gelhar* are consistently lower than field estimates. The *Rehfeldt and Gelhar* term depends on the power of the gradient spectrum only at zero frequency. They imply that higher frequency energy (e.g. periodicity) produces no real mixing. We hypothesize that by ignoring periodicity (and in fact removing it from their data), *Rehfeldt and Gelhar* did not account for a potentially important mixing effect; one that had been previously documented by *Goode and Konikow* [1990]. *Rehfeldt and Gelhar* contend that periodicity can be accounted for in the mean flow equations. This implies that the mean velocity, and as a result, the macrodispersivity would also exhibit periodicity. Yet the dispersivity values *Rehfeldt and Gelhar* use to compare with their approximation were obtained by assuming a constant flow velocity, and are estimates for a constant (large time) macrodispersivity.

A different approach to quantifying macrodispersivity in a variable flow field was taken by *Goode and Konikow* [1990]. They studied the effect of a periodic, discretely varying flow direction on plume spreading. They assumed that the "true" dispersivities were constant well-defined aquifer properties (equivalent to the steady macrodispersivities predicted by stochastic theory) and that an alternating flow direction resulted in "apparent" dispersivities. They related the "apparent" dispersivities to the "true" dispersivities, without addressing the possible effects of geologic variability. The approach taken in this thesis explicitly recognizes the importance of heterogeneity, and shows that *both* geologic and hydrologic variability are important for determining macrodispersivity values.

Like in *Rehfeldt and Gelhar*, the approach taken here relates the macrodispersivity to two fundamental, random quantities: hydraulic conductivity and hydrologic controls (manifested in the hydraulic gradient). Since macrodispersivity is more of a practical measure than a fundamental property, we are interested, like *Goode and Konikow*, in

making the measure applicable to standard moment analysis and transport modeling techniques. Accordingly, we treat periodicity in hydrologic controls as a deviation from the long-term mean. The constant, long term mean gradient is used in the effective conductivity relationship to produce a constant mean velocity. The computed macrodispersivity values are then independent of time and are practical for comparison with moment analyses.

However, we must remember that the quantities of interest: concentration, velocity, head, and conductivity, are represented by ensemble statistics in our stochastic development. We have implied that ergodicity holds, so that the ensemble statistics are appropriate for describing aquifer processes of considerable spatial and temporal extent. With this ergodic hypothesis in mind, one would not expect seasonal flow variations to affect a plume over a short time period. Only after the plume has experienced many realizations of the underlying random processes will its characteristics be adequately described by the effective velocity and macrodispersivity predicted by stochastic theory. When seasonal periodicity is viewed as random (as it is here), rather than as deterministic, then we expect the stochastic results to be most applicable after a travel time of several years.

In order to use the theory presented here, information on the gradient statistics must be obtained. Section 3 of this thesis shows how such statistics can be estimated with measurements of the flow boundary conditions and a numerical flow model. The macrodispersive process is thus related to the most fundamental quantities that describe an aquifer (from a hydrogeologist's point of view): the hydraulic conductivity field and the hydrologic controls.

Section 4 shows that for a case where geologic and hydrologic variability are large, the transverse and off-diagonal macrodispersivities predicted by (2.50) are significantly larger than those of *Rehfeldt and Gelhar* or *Gelhar and Axness*. However, in many field situations (e.g. low flow variability, high conductivity), the earlier theories provide a reasonable approximation of the total macrodispersivity.

The mathematical development of this thesis builds on the earlier works of *Gelhar and Axness* and *Rehfeldt and Gelhar*, with similar assumptions and stochastic methods. Like in *Rehfeldt and Gelhar* [1992, equation 16] the gradient of head is decomposed into three terms:

$$\frac{\partial h(\mathbf{x},t)}{\partial x_i} = -\overline{J_i} - J'_{bi}(t) + \frac{\partial h'_f(\mathbf{x},t)}{\partial x_i} \tag{5.1}$$

with each term being more explicitly defined here (see Table 2.1). The major modification to *Rehfeldt and Gelhar* is the inclusion of the term $J'_{bi}f'$ in the Darcy perturbation equation to handle gradient fluctuations that are large compared to the mean gradient. The resulting macrodispersivity expression (2.50) has a third term, $A_{ij}^{(st)}$, that depends on the log-conductivity *and* hydraulic gradient statistics. This third term can be important at heterogeneous sites with a highly variable gradient—a rather common scenario.

REFERENCES

Ababou, R., Three-dimensional flow in random porous media, Ph.D., Mass. Inst. of Tech., 1988.

Aris, R., On the dispersion of a solute in a fluid flowing through a tube, *Proc. R. Soc. London Ser. A, 235*, 67-78, 1956.

Bear, J., *Dynamics of Fluids in Porous Media*. Elsevier/Dover, New York, 1972.

Garabedian, S. P., D. R. Leblanc, L. W. Gelhar, and M. A. Celia, Large scale natural gradient tracer test in sand and gravel, Cape Cod, Massachusetts, 2. Analysis of spatial moments for a nonreactive tracer, *Water Resources Research, 27*, 911-924, 1991.

Gelhar, L. W., and C. L. Axness, Three-dimensional stochastic analysis of macrodispersion in aquifers, *Water Resources Research, 19*, 161-180, 1983.

Gelhar, L. W., Stochastic subsurface hydrology: From theory to applications, *Water Resources Research, 22*, 135S-145S, 1986.

Gelhar, L. W., C. Welty, and K. R. Rehfeldt, A critical review of data on field-scale dispersion in aquifers, *Water Resources Research, 28*, 1955-1974, 1992.

Gelhar, L. W., *Stochastic Subsurface Hydrology*. Prentice-Hall, Englewood Cliffs, NJ, 1993.

Goode, D. J., and L. F. Konikow, Apparent dispersion in groundwater flow, *Water Resources Research, 26*, 2339-2351, 1990.

Kinzelbach, W., and P. Ackerer, Modelisation de la propagation d'un contaminant dans un champ d'ecolement transitoire, *Hydrogeologie, 2*, 197-205, 1986.

LeBlanc, D. R., S. P. Garabedian, K. M. Hess, L. W. Gelhar, R. D. Quadri, K. G. Stollenwerk, and W. G. Wood, Large-scale natural gradient tracer test in sand and gravel, Cape Cod, Massachusetts, 1. Experimental design and observed tracer movement, *Water Resources Research, 27*, 895-910, 1991.

Li, S.-G., and D. McLaughlin, A nonstationary spectral method for solving stochastic groundwater problems: Unconditional analysis, *Water Resources Research, 27*, 1589-1605, 1991.

Linderfelt, W .R., and J. L. Wilson, Field study of capture zones in a shallow sand aquifer, in *Transport and Reactive Processes in Aquifers*, edited by Dracos and Stauffer, pp. 289-294, Balkema, Rotterdam, 1994.

Naff, R. L., and A. V. Vecchia, Stochastic analysis of three-dimensional flow in a bounded domain, *Water Resources Research, 22*, 695-704, 1986.

Naff, R. L., T.-C. J. Yeh, and M. W. Kemblowski, Reply, *Water Resources Research, 25*, 2523-2525, 1989.

Papoulis, A., *Probability, Random Variables, and Stochastic Processes*. McGraw-Hill, New York, 1984.

Rehfeldt, K. R., and L. W. Gelhar, Stochastic analysis of dispersion in unsteady flow in heterogeneous aquifers, *Water Resources Research, 28*, 2085-2099, 1992.

APPENDIX A. NOTATION

(Note: Also refer to Table 2.1)

DEFINITIONS

z_i	i^{th} component of a vector **z**
z	magnitude of $\overline{z_i}$
B_{ij}	i,j^{th} component of the tensor **B**
δ_{ij}	(Kronecker delta) equal to 1 if $i = j$; 0 otherwise
$\delta(\mathbf{x}-\mathbf{y})$	(Dirac delta function) $\int \delta(\mathbf{x}-\mathbf{y}) f(\mathbf{x}) d\mathbf{x} = f(\mathbf{y})$
i	$\sqrt{-1}$
$S_{z_i z_j}$	spectrum of components z_i' and z_j'
W_{z_i}	Fourier amplitude associated with z_i'
$W_{z_i}^*$	complex conjugate of W_{z_i}

VARIABLES

a_H	amplitude for the harmonic part of the H process (L)
A_{ij}	(total) macrodispersivity tensor (L^2/T)
$A_{ij}^{(s)}$	macrodispersivity from spatial heterogeneity only (L^2/T)
$A_{ij}^{(t)}$	macrodispersivity from temporal gradient variability only (L^2/T)
$A_{ij}^{(st)}$	macrodispersivity from interaction between spatial and temporal variations (L^2/T)
c	solute concentration (M/L^3)
E_{ij}	local bulk dispersion tensor (L^2/T)

G_j	mean concentration gradient (M/L^2), equal to $-\partial\bar{c}/\partial x_j$ (M/L^4)
f	log-conductivity
h	hydraulic head (L)
H	boundary head (L)
J_i	hydraulic gradient
K	hydraulic conductivity (L/T)
K_g	geometric mean of hydraulic conductivity (L/T)
$\hat{K}_{ij}$	effective conductivity tensor (L/T)
λ_f	correlation scale of log-conductivity (L)
λ_H	correlation time scale for a Markov H process (T)
m_i	sensitivity of the gradient to boundary fluctuations (L^{-1})
n	aquifer porosity
q_i	specific discharge or Darcy velocity vector (L/T)
σ_f^2	log-conductivity variance
σ_H^2	variance of a Markov H process (L^2)
S_s	specific storage (L^{-1})
v	mean pore velocity (L/T), equal to q/n
ω_0	characteristic angular frequency for a harmonic H process (radians/T)

APPENDIX B. SIMPLIFICATION OF THE MACRODISPERSIVITY INTEGRAL

From (2.56), the general expression for macrodispersivity in an isotropic medium is

$$A_{ij}^{(st)} = \frac{K_g^2}{q}\int\left(\delta_{il} - \frac{k_i k_l}{k^2}\right)\left(\delta_{jm} - \frac{k_j k_m}{k^2}\right)\{P_{lm}\}S_{ff}(k)d\mathbf{k} \tag{B.1}$$

with

$$P_{lm} = \int_{-\infty}^{\infty} \frac{S_{J_l J_m}(\omega)d\omega}{ni\omega + ik_i\overline{q_i} + k_i k_j E_{ij}} \tag{B.2}$$

For convenience the local dispersion (later taken to zero) is assumed to be isotropic. Thus

$$E_{ij} = E\delta_{ij} \tag{B.3}$$

and

$$P_{lm} = \int_{-\infty}^{\infty} \frac{S_{J_l J_m}(\omega)d\omega}{ni\omega + ik_1 q + k^2 E} \tag{B.4}$$

We solve for P_{lm} following a method similar to *Rehfeldt and Gelhar* [1992, equations 36-40] assuming negligible local dispersion. Multiplying the numerator and denominator of (B.4) by the complex conjugate of the denominator yields

$$P_{lm} = \int_{-\infty}^{\infty} \frac{S_{J_l J_m}(\omega)d\omega\left[-ni\omega - ik_1 q + k^2 E\right]}{(n\omega + k_1 q)^2 + k^4 E^2} \tag{B.5}$$

Dividing the top and bottom of this expression by k^4E^2 and letting

$$v = \frac{n\omega + k_1 q}{k^2 E} \tag{B.6}$$

leads to

$$P_{lm} = \frac{1}{n}\int_{-\infty}^{\infty} S_{J_l J_m}\left(\frac{k^2 Ev - k_1 q}{n}\right)\frac{1-iv}{v^2+1}dv \tag{B.7}$$

Taking the local dispersion to zero gives

$$P_{lm} = \frac{1}{n}\int_{-\infty}^{\infty} S_{J_l J_m}\left(-\frac{k_1 q}{n}\right)\frac{1-iv}{v^2+1}dv \tag{B.8}$$

Considering the case where the gradient is characterized by auto- and cross-spectra that are even in ω yields

$$\begin{aligned} P_{lm} &= \frac{1}{n} S_{J_l J_m}\left(-\frac{k_1 q}{n}\right)\int_{-\infty}^{\infty}\frac{dv}{v^2+1} \\ &= \frac{\pi}{n} S_{J_l J_m}\left(\frac{k_1 q}{n}\right) \end{aligned} \tag{B.9}$$

APPENDIX C. SPECTRAL ANALYSIS OF A LAKE LEVEL TIME SERIES

To quantify the degree of gradient variability at a site, Section 3 proposes the use of a flow model and measurements of the boundary conditions (e.g. H_l, H_u). Here, we look at how the boundary heads are analyzed. Specifically, we are interested in the approximate shape of a head spectrum influenced by both seasonal hydrologic patterns and short duration hydrologic events.

As an example where data are plentiful, consider Ashumet Pond, located near Falmouth, Massachusetts. The United States Geological Survey recorded water levels at the 0.8 square kilometer lake over a 21 year period from December 1972 to January 1994 with successive samples less than 20 days apart on average. The time series of this data is plotted in Figure C.1. The mean lake level for this period was 13.55 meters.

The data were analyzed using the Signal Processing Toolbox of the *Matlab* † numerical computation package. The irregularly spaced data of Figure C.1 were interpolated at every 20th day and the resulting record was used for spectral analysis. Using *Matlab*, the data were sent through a Fast Fourier Transform algorithm, then using a Hanning window, the spectral density function was approximated at discrete frequencies. This approximation is shown in Figure C.2. The procedure is described more thoroughly in the software documentation.

The spectrum of Figure C.2 generally decreases with increasing frequency, with the exception of an increased area of spectral power at around 0.017 radians/day. This frequency corresponds to a one year cycle, confirming our intuition that lake levels are influenced by the seasonal periodicity of natural hydrology, and inspiring our choice of the model spectrum (4.1).

This exercise serves as an example of a particular procedure, and is not meant to apply directly to the hypothetical site of Section 3 or the nominal case of Section 4.

---

† *Matlab*, Version 4.1, The MathWorks, Inc., 1984-1994.

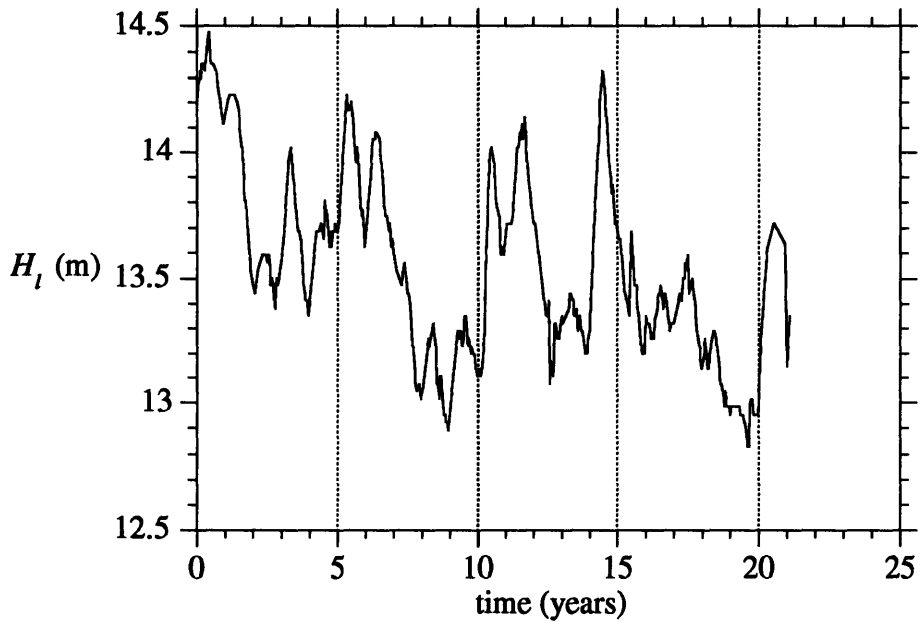

Figure C.1 Record of lake levels at Ashumet Pond (from the United States Geological Survey).

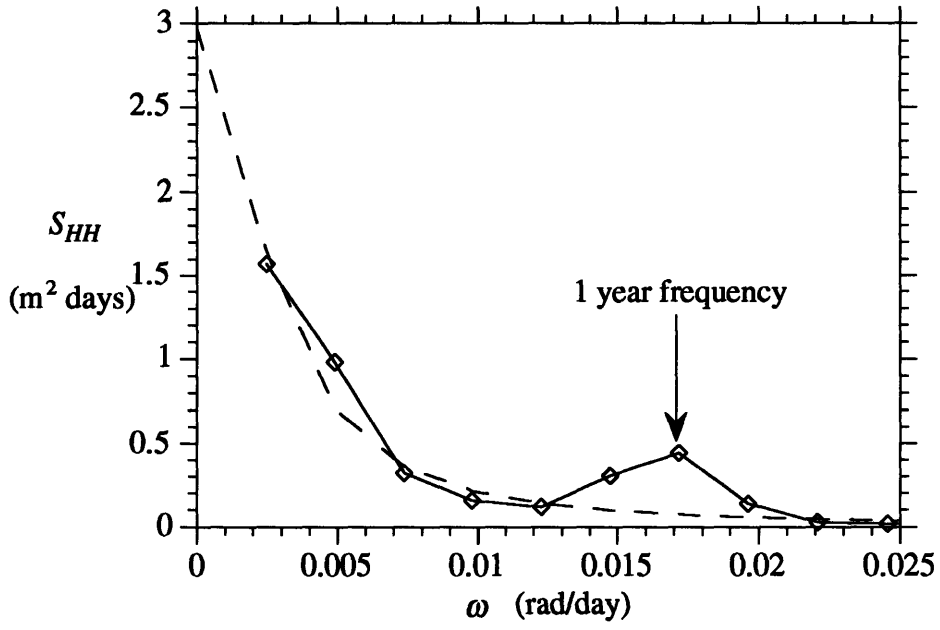

Figure C.2 Estimated spectral density function for the lake level at Ashumet Pond. The dotted line is for a Markov process with a standard deviation of 0.16 m and a correlation scale of 1 year.

APPENDIX D. EVALUATION OF THE MACRODISPERSIVITY INTEGRAL

DIAGONAL TERMS

Recall equations (2.60) and (3.11), and note that if $l \neq m$, $A_{ii}^{(st)}$ is given by

$$A_{ii}^{(st)} = \frac{K_g^2 \pi}{nq} \int \left(\delta_{il} - \frac{k_i k_l}{k^2} \right)^2 m_l^2 S_{HH}\left(\frac{k_1 q}{n}\right) S_{ff}(k) d\mathbf{k} \tag{D.1}$$

with isotropy and negligible local dispersion assumed.

For a log-conductivity field with an isotropic, exponential covariance structure, the spectrum of f is written

$$S_{ff}(k) = \frac{\sigma_f^2 \lambda_f^3}{\pi^2 \left(1 + \lambda_f^2 k^2\right)^2} \tag{D.2}$$

It is convenient to make the following substitutions:

$$u_i = k_i \lambda_f; \quad u^2 = u_1^2 + u_2^2 + u_3^2 \tag{D.3}$$

where λ_f is the conductivity integral scale. This leads to

$$A_{ii}^{(st)} = \frac{K_g^2 \pi}{nq\lambda_f^3} \int \left(\delta_{im} - \frac{u_i u_m}{u^2} \right)^2 m_l m_m S_{HH}\left(\frac{u_1 q}{n\lambda_f}\right) S_{ff}\left(\frac{u}{\lambda_f}\right) d\mathbf{u} \tag{D.4}$$

and

$$S_{ff}\left(\frac{u}{\lambda_f}\right) = \frac{\sigma_f^2 \lambda_f^3}{\pi^2 \left(1 + u^2\right)^2} \tag{D.5}$$

In this appendix analytical expressions are derived and discussed for Markov and harmonic types of boundary spectra S_{HH}. First, the spectra are analyzed separately, then the results for each type are added to represent the result of an input boundary spectra of the form (4.1). A Markov process is defined by its standard deviation (σ_H) and time

scale (λ_H) while a harmonic process is defined by an amplitude (a_H) and a characteristic frequency (ω_0). Their spectra are given by:

$$S_{HH}(\omega) = \frac{\sigma_H^2 \lambda_H}{\pi\left(1+\lambda_H^2\omega^2\right)} \tag{D.6}$$

and

$$S_{HH}(\omega) = \frac{a_H^2}{4}\delta(\omega-\omega_0); \quad \omega \geq 0 \tag{D.7}$$

respectively.

To aid matters further, we will study scenarios when only one slope parameter, m_l is non-zero. Thus, the gradient is assumed to be varying in one component only. In the end, effects on each macrodispersivity component will be summed to arrive at a value for $A_{ii}^{(st)}$.

Markov 1

Consider a Markov input for H, (D.6), with only the x_1 component of the gradient affected.

Making the substitution

$$\rho = \frac{\lambda_H q}{\lambda_f n} = \frac{v}{v_c}; \quad v_c = \frac{\lambda_f}{\lambda_H} \tag{D.8}$$

in (D.6) leads to

$$S_{HH}\left(\frac{u_1 q}{\lambda_f n}\right) = \frac{\sigma_H^2 \lambda_H}{\pi\left(1+\rho^2 u_1^2\right)} \tag{D.9}$$

and

$$A_{ii}^{(st)} = \frac{K_g^2 m_1^2 \sigma_H^2 \sigma_f^2 \lambda_H}{\pi^2 nq} \iiint \left(\delta_{i1} - \frac{u_i u_1}{u^2}\right)^2 \frac{1}{1+\rho^2 u_1^2} \frac{du_1\, du_2\, du_3}{\left(1+u^2\right)^2} \tag{D.10}$$

Now let

$$A_N = m_1^2 \frac{K_g^2 \sigma_H^2}{q^2} \sigma_f^2 \lambda_f = m_1^2 \frac{\sigma_H^2}{J^2} \frac{\sigma_f^2 \lambda_f}{\gamma^2} \tag{D.11}$$

(where $q_i = \gamma K_g J_i$) so that

$$A_{ii}^{(st)} = A_N \frac{\rho}{\pi^2} \iiint \left(\delta_{i1} - \frac{u_i u_1}{u^2} \right)^2 \frac{1}{1+\rho^2 u_1^2} \frac{du_1\, du_2\, du_3}{\left(1+u^2\right)^2} \tag{D.12}$$

The longitudinal and horizontal components are then

$$A_{11}^{(st)} = A_N \frac{\rho}{\pi^2} \iiint \left(1 - \frac{u_1^2}{u^2} + \frac{u_1^4}{u^4} \right) \frac{1}{1+\rho^2 u_1^2} \frac{du_1\, du_2\, du_3}{\left(1+u^2\right)^2} \tag{D.13}$$

$$A_{22}^{(st)} = A_N \frac{\rho}{\pi^2} \iiint \left(\frac{u_1^2 u_2^2}{u^4} \right) \frac{1}{1+\rho^2 u_1^2} \frac{du_1\, du_2\, du_3}{\left(1+u^2\right)^2} \tag{D.14}$$

Converting to spherical coordinates with the following transformation:

$$u_1 = u\cos\phi;\ u_2 = u\sin\phi\cos\theta;\ u_3 = u\sin\phi\sin\theta \tag{D.15}$$

and taking advantage of symmetry gives

$$A_{11}^{(st)} = A_N \frac{8\rho}{\pi^2} \int_0^{\frac{\pi}{2}} \int_0^{\frac{\pi}{2}} \left(1 - 2\cos^2\phi + \cos^4\phi\right) \sin\phi\, [Q]\, d\phi\, d\theta \tag{D.16}$$

$$A_{22}^{(st)} = A_N \frac{8\rho}{\pi^2} \int_0^{\frac{\pi}{2}} \int_0^{\frac{\pi}{2}} \left(\cos^2\phi \sin^3\phi \cos^2\theta\right) [Q]\, d\phi\, d\theta \tag{D.17}$$

with

$$Q = \int_0^{\infty} \frac{u^2\, du}{\left(1+\rho^2\cos^2\phi\, u^2\right)\left(1+u^2\right)^2} \tag{D.18}$$

With the help of the symbolic math software *Maple*†, Q is evaluated to

$$Q = \frac{\pi}{4(1+\rho\cos\phi)^2} \tag{D.19}$$

Substituting this value for Q and performing the θ integration gives

$$A_{11}^{(st)} = A_N \rho \int_0^{\frac{\pi}{2}} \frac{\left(\sin\phi - 2\cos^2\phi\sin\phi + \cos^4\phi\sin\phi\right)}{(1+\rho\cos\phi)^2} d\phi \tag{D.20}$$

$$A_{22}^{(st)} = A_N \frac{\rho}{2} \int_0^{\frac{\pi}{2}} \frac{\cos^2\phi\sin^3\phi}{(1+\rho\cos\phi)^2} d\phi \tag{D.21}$$

These integrals are evaluated using another symbolic math program, *Mathematica*‡, to yield

$$A_{11}^{(st)} = A_N \left[\frac{12\rho - 6\rho^2 - 8\rho^3 + 3\rho^4 - 12\ln(1+\rho) + 12\rho^2\ln(1+\rho)}{3\rho^4} \right] \tag{D.22}$$

$$A_{22}^{(st)} = A_{33}^{(st)} = A_N \left[\frac{-6\rho + 3\rho^2 + \rho^3 + 6\ln(1+\rho) - 3\rho^2\ln(1+\rho)}{3\rho^4} \right] \tag{D.23}$$

where it is noted that the two transverse components are equal.

Markov 2

The same process is followed when only J_2 varies, with

$$A_N = m_2^2 \frac{K_g^2\sigma_H^2}{q^2}\sigma_f^2\lambda_f = m_2^2 \frac{\sigma_H^2}{J^2}\frac{\sigma_f^2\lambda_f}{\gamma^2} \tag{D.24}$$

and

---

† *Maple V*, Release 3, Waterloo Maple Software, 1981-1994.

‡ *Mathematica*, Version 2.2 for the X Window System, Wolfram Research, Inc., Champaign, Ill., 1993.

$$A_{ii}^{(st)} = A_N \frac{\rho}{\pi^2} \iiint \left(\delta_{i2} - \frac{u_i u_2}{u^2} \right)^2 \frac{1}{1+\rho^2 u_1^2} \frac{du_1\, du_2\, du_3}{\left(1+u^2\right)^2} \tag{D.25}$$

In spherical coordinates, the three components of macrodispersivity are

$$A_{11}^{(st)} = A_N \frac{8\rho}{\pi^2} \int_0^{\frac{\pi}{2}} \int_0^{\frac{\pi}{2}} \left(\cos^2\phi \sin^3\phi \cos^2\theta \right) [Q]\, d\phi\, d\theta \tag{D.26}$$

$$A_{22}^{(st)} = A_N \frac{8\rho}{\pi^2} \int_0^{\frac{\pi}{2}} \int_0^{\frac{\pi}{2}} \left(1 + 2\sin^2\phi \cos^2\theta + \sin^4\phi \cos^4\theta \right) \sin\phi\, [Q]\, d\phi\, d\theta \tag{D.27}$$

$$A_{33}^{(st)} = A_N \frac{8\rho}{\pi^2} \int_0^{\frac{\pi}{2}} \int_0^{\frac{\pi}{2}} \left(\sin^5\phi \sin^2\theta \cos^2\theta \right) [Q]\, d\phi\, d\theta \tag{D.28}$$

with Q defined in (D.18) and (D.19).

Once θ integration is performed, the ϕ integrals are solved with the help of *Mathematica* to give

$$A_{11}^{(st)} = A_N \left[\frac{-6\rho + 3\rho^2 + \rho^3 + 6\ln(1+\rho) - 3\rho^2 \ln(1+\rho)}{3\rho^4} \right] \tag{D.29}$$

$$\begin{aligned} A_{22}^{(st)} = A_N \Bigg[& \frac{\rho}{1+\rho} - \frac{-2\rho + \rho^2 + 2\ln(1+\rho)}{\rho^2} \\ & + \frac{12\rho - 6\rho^2 - 8\rho^3 + 3\rho^4 - 12\ln(1+\rho) + 12\rho^2 \ln(1+\rho)}{8\rho^4} \Bigg] \end{aligned} \tag{D.30}$$

$$A_{33}^{(st)} = \left[\frac{12\rho - 6\rho^2 - 8\rho^3 + 3\rho^4 - 12\ln(1+\rho) + 12\rho^2 \ln(1+\rho)}{24\rho^4} \right] \tag{D.31}$$

Harmonic 1

Now consider a harmonic input (D.7) with only J_1 being affected. The following substitutions are made in the integral expression (D.4):

$$\omega' = \frac{u_1 q}{\lambda_f n};\quad \rho = \frac{q}{n\lambda_f \omega_0} = \frac{v}{v_c};\quad v_c = \lambda_f \omega_0 \tag{D.32}$$

$$u^2 = \left(\frac{\omega'^2}{\rho\omega_0}\right)^2 + r^2;\quad r^2 = u_2^2 + u_3^2 \tag{D.33}$$

(note that ρ is defined differently in the Markov and harmonic cases) These substitutions give

$$A_{11}^{(st)} = A_N \frac{2}{\pi} \int_0^\infty\int_0^\infty\int_0^\infty \left(1 - \frac{(\omega'/\rho\omega_0)^2}{(\omega'/\rho\omega_0) + r^2}\right)^2 \frac{\delta(\omega - \omega')}{\left(1 + (\omega'/\rho\omega_0)^2 + r^2\right)^2} d\omega'\, du_2\, du_3 \tag{D.34}$$

$$A_{22}^{(st)} = A_N \frac{2}{\pi} \int_0^\infty\int_0^\infty\int_0^\infty \left(\frac{u_2(\omega'/\rho\omega_0)}{(\omega'/\rho\omega_0) + r^2}\right)^2 \frac{\delta(\omega - \omega')}{\left(1 + (\omega'/\rho\omega_0)^2 + r^2\right)^2} d\omega'\, du_2\, du_3 \tag{D.35}$$

with

$$A_N = m_1^2 \frac{K_g^2 a_H^2 \sigma_f^2 \lambda_f}{q^2} = m_1^2 \frac{a_H^2}{J^2} \frac{\sigma_f^2 \lambda_f}{\gamma^2} \tag{D.36}$$

Making the substitutions

$$u_2 = r\cos\theta;\quad u_3 = r\sin\theta \tag{D.37}$$

and integrating over ω' and θ leads to the following forms:

$$A_{11}^{(st)} = A_N \int_0^\infty \left(1 - \frac{2\rho^{-2}}{\rho^{-2} + r^2} + \frac{\rho^{-4}}{\left(\rho^{-2} + r^2\right)^2}\right) \frac{r\, dr}{\left(1 + \rho^{-2} + r^2\right)^2} \tag{D.38}$$

$$A_{22}^{(st)} = \frac{A_N}{2} \int_0^\infty \left(\frac{\rho^{-2} r^2 \cos^2\theta}{\rho^{-2} + r^2}\right) \frac{r\, dr}{\left(1 + \rho^{-2} + r^2\right)^2} \tag{D.39}$$

These are integrated with *Mathematica*, leading to the following results:

$$A_{11}^{(st)} = A_N\left[\frac{2\rho^2+\rho^4-2\ln\left(1+\rho^2\right)-2\rho^2\ln\left(1+\rho^2\right)}{2\rho^4}\right] \tag{D.40}$$

$$A_{22}^{(st)} = A_{33}^{(st)} = A_N\left[\frac{-2\rho^2+2\ln\left(1+\rho^2\right)+\rho^2\ln\left(1+\rho^2\right)}{4\rho^4}\right] \tag{D.41}$$

Harmonic 2

The procedure for handling the harmonic spectrum affecting only J_2 is quite similar to the developments in (D.32) through (D.41). This time

$$A_N = m_1^2\frac{K_g^2 a_H^2\sigma_f^2\lambda_f}{q^2} = m_1^2\frac{a_H^2}{J^2}\frac{\sigma_f^2\lambda_f}{\gamma^2} \tag{D.42}$$

and the integrands differ slightly.

The resulting expressions for $A_{ii}^{(st)}$ are

$$A_{11}^{(st)} = A_N\left[\frac{-2\rho^2+2\ln\left(1+\rho^2\right)+\rho^2\ln\left(1+\rho^2\right)}{4\rho^4}\right] \tag{D.43}$$

$$A_{22}^{(st)} = A_N\left[\frac{6\rho^2+\rho^4+3\rho^6-6\ln\left(1+\rho^2\right)-4\rho^2\ln\left(1+\rho^2\right)+2\rho^4\ln\left(1+\rho^2\right)}{16\rho^4\left(1+\rho^2\right)}\right] \tag{D.44}$$

$$A_{33}^{(st)} = A_N\left[\frac{2\rho^2+\rho^4-2\ln\left(1+\rho^2\right)-2\rho^2\ln\left(1+\rho^2\right)}{16\rho^4}\right] \tag{D.45}$$

General $A_{ii}^{(st)}$

Using the results above, but noting that A_N is defined differently in the scenarios, the total $A_{ii}^{(st)}$ is now written as:

$$A_{ii}^{(st)} = \frac{\sigma_f^2\lambda_f}{\gamma^2}\left[\frac{\sigma_H^2}{J^2}\left(m_1^2 A_{ii}^*\big|_{M1} + m_2^2 A_{ii}^*\big|_{M2}\right) + \frac{a_H^2}{J^2}\left(m_1^2 A_{ii}^*\big|_{H1} + m_2^2 A_{ii}^*\big|_{H2}\right)\right] \tag{D.46}$$

where $A_{11}^*\big|_{M1}$ is the term in brackets in (D.22), $A_{11}^*\big|_{M2}$ is the bracketed term in (D.29), etc. Thus the general $A_{ii}^{(st)}$ is a function of σ_H, a_H, J, m_1, m_2, v, λ_f, σ_f, γ, and ω_0. The function given by (D.46) is used in Figures 4.2-4.7.

OFF-DIAGONAL TERMS

We now consider the possibility of non-zero off-diagonal terms resulting from variability in *both* components of the hydraulic conductivity. Considering cases when $i \neq j$, and m_1 and m_2 are non-zero, the integral (D.4) can be reduced (with even/odd arguments) to

$$A_{12}^{(st)} = A_{21}^{(st)} = m_1 m_2 \frac{K_g^2 \pi}{nq\lambda_f^3} \int \left(1 - \frac{u_1^2}{u^2} - \frac{u_2^2}{u^2} + \frac{u_1^2 u_2^2}{u^4}\right) S_{HH}\left(\frac{u_1 q}{\lambda_f n}\right) S_{ff}\left(\frac{u}{\lambda_f}\right) d\mathbf{u} \tag{D.47}$$

$$A_{13}^{(st)} = A_{23}^{(st)} = A_{31}^{(st)} = A_{32}^{(st)} = 0$$

Markov

The Markov spectrum result can be evaluated by making the substitution (D.8), and converting to spherical coordinates. The result is:

$$A_{12}^{(st)} = A_N \frac{8\rho}{\pi^2} \int_0^{\frac{\pi}{2}} \int_0^{\frac{\pi}{2}} \left(1 - \cos^2\phi - \sin^2\phi\cos^2\theta + \cos^2\phi\sin^2\phi\cos^2\theta\right) \sin\phi [Q] d\phi\, d\theta \tag{D.48}$$

with

$$A_N = m_1 m_2 \frac{\sigma_H^2}{J^2} \frac{\sigma_f^2 \lambda_f}{\gamma^2} \tag{D.49}$$

and Q given in (D.18) and (D.19).

Using *Mathematica*, the resulting expression for the off-diagonal term is:

$$\begin{aligned} A_{12}^{(st)} = A_N \Bigg[& \frac{\rho}{1+\rho} - \frac{2\rho + \rho^2 - 2\ln(1+\rho) - 2\rho\ln(1+\rho)}{\rho^2(1+\rho)} \\ & - \frac{-2\rho + \rho^2 + 2\ln(1+\rho)}{2\rho^3} \\ & + \frac{2\left(-6\rho + 3\rho^2 + \rho^3 + 6\ln(1+\rho) - 3\rho^2\ln(1+\rho)\right)}{3\rho^4} \Bigg] \end{aligned} \tag{D.50}$$

Harmonic

Following procedures similar to (D.32) through (D.41), the off-diagonal term resulting from a harmonic head input is

$$A_{12}^{(st)} = A_N\left[\frac{\rho^2}{2+2\rho^2} - \frac{-\rho^2+\ln(1+\rho^2)+\rho^2\ln(1+\rho^2)}{2\rho^2(1+\rho^2)} - \frac{\rho^2-\ln(1+\rho^2)}{4\rho^2} + \frac{-2\rho^2+2\ln(1+\rho^2)+\rho^2\ln(1+\rho^2)}{2\rho^4}\right] \tag{D.51}$$

with

$$\rho = \frac{q}{n\lambda_f\omega_0} \tag{D.52}$$

and

$$A_N = m_1 m_2 \frac{a_H^2}{J^2}\frac{\sigma_f^2\lambda_f}{\gamma^2} \tag{D.53}$$

General Off-Diagonal Terms

The Markov and Harmonic results are combined to represent the spectrum of (4.1), with the general off-diagonal terms given by:

$$A_{12}^{(st)} = A_{12}^{(st)} = m_1 m_2\left(\frac{\sigma_H^2}{J^2}A_{12}^*\Big|_M + \frac{a_H^2}{J^2}A_{12}^*\Big|_H\right) \tag{D.54}$$

where the starred terms are the bracketed sums in (D.50) and (D.51), respectively (with the respective definitions for ρ).